Dual-Targeting and Stimuli-Triggered Liposomal Drug Delivery in Cancer Treatment

Nour AlSawaftah[1], William G. Pitt[2], and Ghaleb A. Husseini[1,*]

[1]Department of Chemical Engineering, American University of Sharjah, Sharjah, UAE

[2]Chemical Engineering Department, Brigham Young University, Utah, USA

*Corresponding author: ghusseini@aus.edu

Abstract

The delivery of chemotherapeutics to solid tumors using smart drug delivery systems (SDDSs) takes advantage of the unique physiology of tumors (i.e., disordered structure, leaky vasculature, abnormal extracellular matrix (ECM), and limited lymphatic drainage) to deliver anti-cancer drugs with reduced systemic side effects. Liposomes are the most promising of such SDDSs and have been well investigated for cancer therapy. To improve the specificity, bioavailability and anti-cancer efficacy of liposomes at the diseased sites, other strategies such as targeting ligands and stimulus-sensitive liposomes have been developed. This review highlights relevant surface functionalization techniques and stimuli-mediated drug release for enhanced delivery of anti-cancer agents at tumor sites, with a special focus on dual functionalization and design of multi-stimuli responsive liposomes.

Introduction

Cancer is the second leading cause of noncommunicable disease (NCD) deaths globally, causing approximately 9 million deaths annually [1]. According to the American Cancer Society (ACS), in the year 2021, an estimated 1.9 million new cancer cases are expected to be diagnosed, and over 600 thousand deaths will be caused by the disease in the United States alone [2]. The principal treatment strategies against cancer include surgery, chemotherapy, radiation therapy, and hormone therapy. Surgery can be used to determine whether a certain mass is cancerous, determine the extent of cancer, excise cancerous masses, and reconstruct tissues and organs affected by cancer.

Radiation therapy is another common technique used to treat nonmetastatic malignancies. Radiotherapy involves destroying cancer cells using high-energy particles or waves (e.g., x-rays, gamma

rays). In contrast to surgery and radiation, chemotherapy is used to treat cancer throughout the whole body, making it an invaluable tool for the treatment of disseminated or metastatic cancer. On the other hand, hormone therapy can only be used in the treatment of hormone-sensitive types of cancer and aims to stop hormone synthesis and prevent hormone-positive effects on cancer cells [3–5].

The aforementioned treatments are often accompanied by adverse side effects, such as fatigue, hair loss, infections, pain, nausea, mucositis, and vomiting, that can significantly reduce cancer patients' quality of life. In recent years, a wide range of drug delivery systems (DDSs) has been developed to improve cancer therapies [3,6,7]. DDSs are nanoplatforms capable of delivering therapeutic agents to the diseased area and releasing their contents in response to an internal (e.g., temperature, pH, enzymes) or external trigger (e.g., temperature, light, mechanical waves, electric and magnetic fields). A variety of DDSs has been developed, including micelles, dendrimers, liposomes, solid nanoparticles, carbon nanotubes (CNTs), silica nanoparticles, and quantum dots (QDs) [8,9]. Liposomes are among the most successful DDSs and have found numerous applications in targeted drug delivery. In this review, we will focus on recent developments pertaining to the use of liposomes in cancer treatment, particularly on the use of active targeting mechanisms and stimuli-responsive targeting.

Passive and Active Targeting

Before nanocarriers reach their targeted sites, they need to overcome several biological barriers created by the host immune system, in addition to the abnormal tumor physiology, which includes defective vasculature, abnormal ECM, and high interstitial fluid pressure. Therefore, the physical and chemical properties of nanoparticles (NPs) are of particular importance in drug delivery applications. The size and shape of NPs are important in determining the NPs' circulation time and targeting within the body [10]. Particles with diameters greater than 150 nm are detected by organs of the reticuloendothelial system (RES), while particles with a diameter smaller than 100 nm will remain within the fenestrae of the endothelial lining of blood vessels, hence reducing the possibility of being recognized and phagocytized. As for shape, studies have reported that spherically shaped particles are internalized more easily than NPs of other shapes [3,10]. Moreover, hydrophobicity, surface charge, and surface ligands influence the NPs' behavior *in vivo* and produce significant changes in their performance.

Tumor vasculature is often defective and leaky, with wide fenestrations between cells and limited lymphatic drainage. These factors allow the accumulation of NPs within the tumor interstitium, a phenomenon known as the enhanced permeability and retention (EPR) effect [11–13]. Passive targeting uses the unique pathophysiology of tumor vessels as well as the EPR effect to enable the accumulation of nanocarriers at tumor sites. Active targeting can significantly increase the amount of drug delivered to the tumor site compared to passively targeted NPs. It entails specific interactions between the targeted cells

and the drug carrier through receptor-ligand interactions. Some receptors are often overexpressed on tumor cells; therefore, surface-modified nanocarriers displaying complementary ligands will recognize and bind to these cells' receptors (refer to Figure 1). The formed complex is then internalized through receptor-mediated endocytosis, thereby enhancing cellular uptake and facilitating drug release inside the cell [3,11,12].

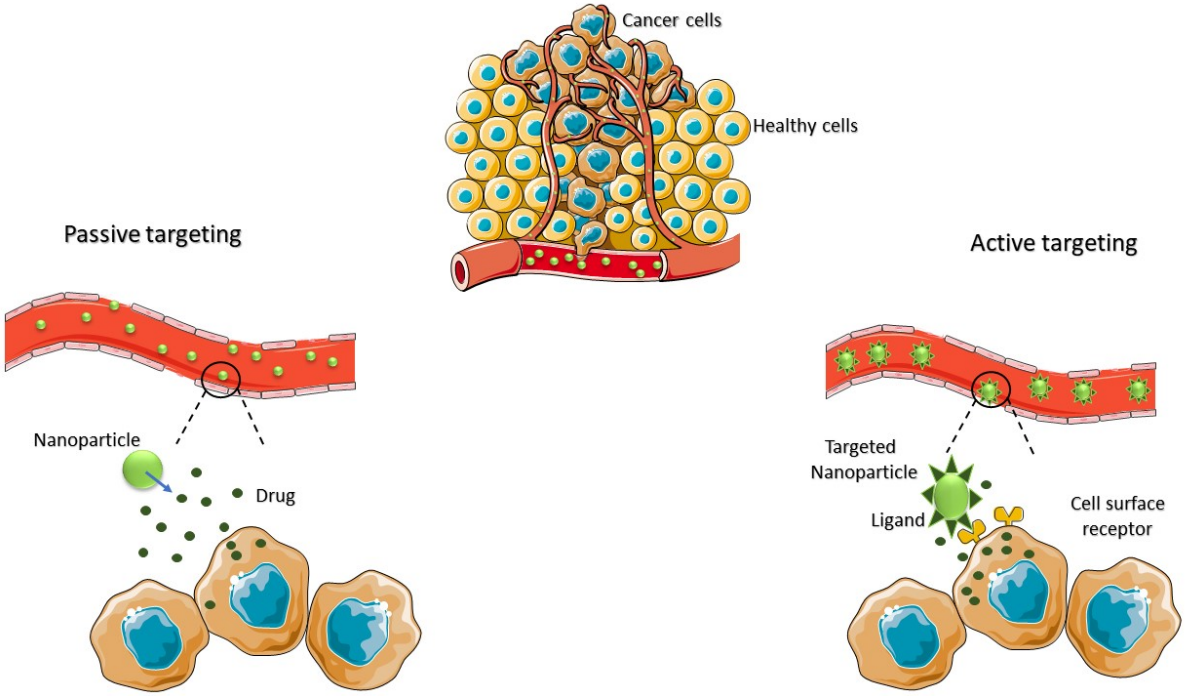

Figure 1. Passive and active targeting of tumors.

Liposomes

The use of liposomes in targeted drug delivery has been thoroughly investigated. Liposomes were first developed by Alec Bangham in the early 1960s [14] when he noticed that phospholipids naturally form vesicles when dispersed in an aqueous medium. Ever since their discovery, liposomes have been used in numerous applications. Liposomes are concentric spherical vesicles consisting of one or more lipid bilayers surrounding an aqueous core. Within a bilayer, the hydrophilic heads of the phospholipids are directed outwards (to the aqueous phase), while the hydrophobic tails are directed into the membrane interior. The amphipathic nature of liposomes enables them to entrap both hydrophilic and hydrophobic drugs within the aqueous interior and the membrane, respectively. Liposomes offer several advantages over other nanocarrier systems; these include biocompatibility, biodegradability, non-immunogenicity, enhancing drug solubility, sustained drug release, reducing the toxic effect of drugs, increasing drug concentration at the target site, aiding in overcoming multidrug resistance (MDR), as well as improving the therapeutic index of the entrapped drug [15,16].

Liposomes can be categorized according to structure, composition, and preparation method. Based on structure, liposomes are divided into unilamellar, multilamellar, and multivesicular. In terms of composition, liposomes can be classified into conventional, fusogenic, long circulatory, pH-sensitive, ionic, magnetic, heat-sensitive, and immunoliposomes (refer Figure 2) [16]. The choice of liposomal preparation method depends on the membrane components' physicochemical properties, the payload, and the dispersing medium [17,18].

Techniques for liposomes preparation are divided into mechanical dispersion methods (e.g., lipid film hydration, sonication, micro-emulsification, French pressure cell, membrane extrusion, and freeze-thawing), solvent dispersion methods (e.g., ethanol/ether injection, double emulsion, and reverse-phase evaporation) and detergent solubilization (e.g., dialysis, column chromatography, and dilution) [16,18].

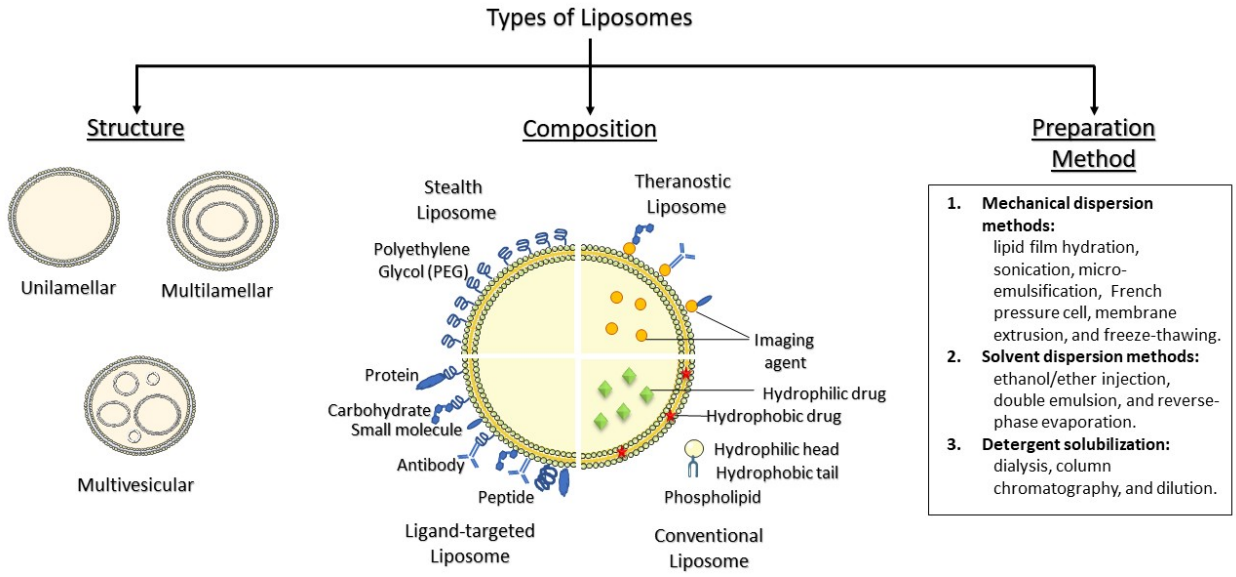

Figure 2. Classification of liposomes based on size, structure, and preparation method.

Liposome Surface Functionalization

Functionalization of liposomes using poly-ethylene glycol (PEG)

Drug delivery applications necessitate extended circulation times, which means that liposomes must evade detection and clearance by organs of the RES. This desired invisibility can be imparted onto liposomes by decorating their surfaces with molecular groups or polymers that suppress opsonization by

plasma proteins; these liposomes are known as “stealth liposomes.” The most commonly used polymeric substance is poly-ethylene glycol (PEG) [3,19].

PEG is a highly biocompatible, nonimmunogenic synthetic, linear polyether diol characterized by ease of synthesis, high flexibility, and aqueous/organic solubility. The presence of PEG on the surface of liposomes helps extend their blood circulation time, reduce their uptake by the RES, enhance the stability of the formulations and improve their distribution in the targeted area [20,21].

Functionalization of liposomes using targeting ligands

Active targeting was defined earlier as the modification of NPs with targeting moieties, enabling them to recognize and bind to target cells through ligand-receptor interactions. Active targeting is particularly beneficial in cancer therapy because specific ligand-receptor interactions reduce non-specific interactions that may increase normal tissue toxicity. Actively targeted liposomal systems are made by grafting moieties such as peptides, proteins, monoclonal antibodies, aptamers, carbohydrates, and other small molecules, onto the surface of liposomes. The targeting moiety can be either integrated directly into the lipid membrane or attached to the distal end of the polymeric coating, i.e., PEG [11,19,22].

Folic acid

Folic acid (FA) is a low molecular-weight vitamin used by eukaryotic cells for single-carbon metabolism and the synthesis of nucleotide bases. The cellular uptake of FA can occur either through the reduced folate carrier (RFC) or the folate receptor (FR). The RFC uses membrane carrier proteins to transport folate across the cell membrane. On the other hand, the FR is a glycoprotein receptor that mediates the endocytosis of folate. The RFC is distributed all-over and functions in the uptake of dietary folate. In contrast, the FR has four known isoforms (FR-α, FR-β, FR-γ, and FR-δ) that are upregulated on activated macrophages and cancer cells [23–25]. FR-α is overexpressed in ovarian carcinomas and other epithelial cancers, FR-β is overexpressed in myeloid leukemia, FR-δ is expressed in regulatory T cells, while FR-γ is secreted by the lymphoid cells [25].

Several folate-conjugated liposomal systems have been reported in literature. Moghimipour et al. [26] prepared 5-fluorouracil (5FU)-loaded-FA liposomes. *In vitro* studies were performed using colon carcinoma (CT26) cells, while the anti-tumor activity and tissue toxicity were studied *in vivo*. FA-liposomes showed higher cellular uptake and tumor inhibition than the free drug on cancer cells (88.75 mm^3 and 210.00 mm^3 tumor volumes, respectively). Zhu et al. [27] compared the anti-cancer activity of docetaxel (DTX)-loaded FA-liposomes (LPs-DTX-FA) to that of co-spray-dried LPs-DTX-FA. Although the co-spray-dried liposomes showed higher cellular uptake and cytotoxicity than LPs-DTX-FA, they exhibited less specific tumor targeting. The *in vivo* study results showed a 45-fold higher concentration of DTX in

the lungs of Sprague Dawley rats when tracheal administration was used compared with intravenous administration. The findings of this study showed that co-spray-drying is able to change the properties of the NPs, and that tracheal administration of the dried liposomal formulation gave higher drug exposure at the tumor site.

In another study, Wang et al. [28] synthesized FA-modified curcumin (CUR)-loaded liposomes and evaluated their anti-tumor activity. The characterization of the developed liposomes included particle size, transmission electron microscopy (TEM), and zeta potential. *In vitro* studies using cervical cancer (HeLa cells) were used to determine percent drug entrapment efficiency (%EE), drug-loading (%DL) capacity, growth inhibition, cellular uptake, and release properties. The pharmacodynamics were studied *in vivo* using Balb/c mice. The results of the characterization tests showed that the spherical liposomes had an average diameter of approximately 110.3 nm, and a zeta potential just above −15 mV. The %EE and %DL of developed liposomes were 87.6 % and 7.9 %, respectively. Furthermore, the cellular uptake of the liposomes was enhanced 10 fold when free CUR was compared to FA-LPs/CUR-treated HeLa cells. In the *in vivo* studies, the cytoplasms of tumor cells treated with coumarin-6 labeled FA-modified CUR-LPs showed strong green fluorescence. Additionally, a considerable reduction of the tumor volumes was observed.

Transferrin (Tf)

Iron is an essential cofactor of proteins involved in numerous cellular processes, including oxygen transport, metabolism, production of enzymes, hematopoiesis, and DNA synthesis. Mammals obtain the iron needed to maintain bodily functions from their diets. Transferrin (Tf) is part of a family of proteins that bind to iron and deliver it into cells via interactions with its receptor. Tf is a double-lobed serum glycoprotein secreted by the liver [29]. Iron-free Tf, also known as apo-Tf, can bind to two iron molecules forming diferric or holo-Tf, which in turn binds to transferrin receptors (TfRs). Once bound to the receptor, the complex is internalized into the endosome through receptor-mediated endocytosis, where the acidic environment (pH~5.5) causes structural rearrangements of the Tf-TfR complex inducing iron release. Following iron release, the Tf-TfR complex is recycled to the cell surface where the return to physiological pH (pH~7.4) will dissociate the complex and release Tf for re-use [30].

The TfR family includes TfR1 (also known as CD71) and TfR2 (also known as CD77). TfR1 is a high affinity, ubiquitously expressed receptor in most normal human tissues, while TfR2 is largely restricted to hepatocytes. However, TfR1 expression is much higher on malignant cells than on healthy cells, and its expression can be correlated with tumor stage and cancer progression. The overexpression of TfR1 on cancer cells can be attributed to the rapid proliferation of cancer cells, which entails a higher iron demand

for DNA synthesis and cell cycle progression. The overexpression of the TfR on malignant cells and the necessity for iron in cancer proliferation make TfRs attractive targets for cancer therapy [29–31].

Several Tf-functionalized liposomal systems have been developed for the delivery of chemotherapeutics to tumor cells overexpressing the TfR. Glioblastomas (GBMs) are highly aggressive and infiltrative brain tumors within a therapy-insensitive environment, resistant to aggressive treatments that may include surgical removal, radiation, and chemotherapy. The main hurdle to a successful treatment using chemotherapy is the tight junctions of endothelial cells in the brain and the low permeability of the blood-brain barrier (BBB), which limits the delivery of drugs to the brain. This demands high doses of chemotherapeutics to be administered in order to reach therapeutic concentrations in the brain, which may lead to systemic toxicity.

Since TfRs are overexpressed in GBMs, Jhaveri et al. [32] exploited the active targeting abilities of Tf-modified Resveratrol (Res)-encapsulating liposomes (called Tf-Res-Ls) to treat GBMs. Res-liposomes were found to be stable, with good %DL, and prolonged drug release *in vitro*. Flow cytometry and confocal microscopy were used to study targeted and non-targeted liposomes' internalization into human malignant glioma (U-87 MG) cells. The Tf-Res-Ls exhibited higher apoptosis levels in GBM cells compared to free Res or Res-L. Tumor growth inhibition and survival rate were measured *in vivo*. At the end of the study, the research group observed a 50% reduction in tumor volumes when comparing free Res with Tf-Res-L treated tumors. For the survival analysis, the survival endpoint was defined as the time taken for the tumor volume to reach 1000 mm^3. After 25 days of initiating the treatment, approximately sixty percent of the animals in the Tf-Res-L group had not reached the cut-off volume, whereas only twenty percent of the animals in the free Res and Res-L treatment groups had yet to reach that stage. Sakpakdeejaroen et al. [33] investigated the therapeutic potential of plumbagin entrapped in Tf-conjugated liposomes. *In vitro* study results showed that the encapsulation of plumbagin in Tf-bearing liposomes increased plumbagin uptake by cancer cells in skin melanoma, epidermoid carcinoma, and human glioblastoma multiforme cell lines compared with that observed with the unencapsulated drug solution.

Moghimipour et al. [34] investigated the use of Tf-targeted liposomal 5FU to treat colon cancer. The *in vitro* cytotoxicity of the synthesized liposomes was investigated using the MTT assay on colorectal adenocarcinoma (HT-29) cells *in vitro*, while fibroblasts were used as control cells. The cytotoxicity mechanism of Tf-liposomes was assessed through the production of reactive oxygen species (ROS), release of cytochrome c, and mitochondrial membrane potential. The characterization tests showed that the average size of the targeted liposomes was slightly above 100 nm, and that the encapsulation efficiency was ~ 59%. The findings of the MTT assay revealed that Tf-targeted liposomes had higher cytotoxic activity in comparison to free 5FU and non-targeted liposomes. Also, lower mitochondrial membrane potential and

release of cytochrome c indicated that Tf-liposomes killed cancer cells through the activation of mitochondrial apoptosis pathways.

Antibodies

Monoclonal antibodies (mAbs) and their fragments (fragment antigen-binding (Fab)) are target-recognizing proteins commonly used in cancer drug delivery applications [35,36]. Moreover, single-chain variable (scFv) fragments are fusion proteins composed of a variable region of the heavy and light chains of an antibody connected by a peptide linker [37]. The modification of liposomes with mAbs and Fabs to generate immunoliposomes has been used for targeted delivery in cancer therapy.

Gabbia et al. [38] compared the *in vivo* liver toxicity of stealth immunoliposomes (SIL) and super-stealth immunoliposomes ($SSIL_2$), loaded with doxorubicin (DOX). Standard histological analyses showed that SIL-treated rats exhibited numerous granulomas, whereas the livers of $SSIL_2$-treated animals exhibited only a few isolated granulomas. Khayrani et al. [39] assessed the therapeutic efficacy of glycosylated paclitaxel (gPTX)-loaded liposomes functionalized with anti-CD44 antibody (gPTX-IL). The *in vitro* cytotoxicity of gPTX-IL was tested in SK-OV-3 and OVK18 ovarian cancer cell lines. Anti-tumor activity *in vivo* was evaluated by monitoring loss of body weight and H&E staining of the liver, kidney, and spleen; accordingly, gPTX-IL exhibited the most effective anti-tumor activity.

Zheng et al. [40] synthesized ScFv modified liposomes with an additional C-terminal cysteine residue, to target fibroblast growth factor receptor 3 (FGFR3). RT112 and T24 bladder cancer cell lines were chosen as high FGFR3-expressing and low FGFR3-expressing cell lines, respectively. The lipophilic Dio fluorescent dye was used to label both control and targeted liposomes. Immunoliposome-treated RT112 cells showed more green fluorescence compared to the cells treated with non-targeted liposomes; indicating that immunoliposomes are better at delivering Dio into high FGFR3-expressing RT112 cells.

Peptides

Peptides are short chains of amino acids connected by peptide bonds and are typically distinguished from proteins by their shorter length [41]. Although mAbs have shown potential as tumor-targeting agents; they are limited by their large molecular size, high affinity to antigens leading to poor tumor penetration, and liver and bone marrow toxicity due to non-specific antibody uptake [42]. Peptides can overcome these limitations because they are smaller, and easier to produce and manipulate. Furthermore, peptides have a moderate affinity to antigens, resulting in better tumor penetration compared to antibodies [43–45].

Zhang et al. [46] synthesized β3 integrin specific ligand (B3int)-modified liposomes encapsulating DOX (B3int-LS-DOX). *In vitro* cellular uptake studies were conducted using prostate cancer (PC-3 and DU-145 cell lines). The developed liposome displayed higher uptake in PC-3 cells than in DU-145 cells,

generating a three-fold increase in intracellular DOX in the former. Furthermore, in cell viability assays, B3int-LS-DOX exhibited significant inhibitory effects in PC-3 tumor cells.

In another study, Tang et al. [47] synthesized Gemcitabine (GEM)-loaded RGD modified liposomes (RGD-GEM-LPs). RGD peptides are known to bind preferentially to the $\alpha_v\beta_3$ integrin. The *in vitro* release studies showed that the mechanism of GEM release from both targeted and non-targeted liposomes involved distinct burst release for 30 min after administration. Non-invasive fluorescence imaging was used to monitor the tumor-targeting efficiency of RGD-GEM-LPs in mice bearing SKOV3 ovarian cancer xenografts. The imaging results showed that the uptake of DiD delivered to tumors by RGD-GEM-LPs increased gradually compared to healthy tissues following injection, which suggested that these liposomes were more likely to accumulate in tumors than in normal tissues. The cellular uptake studies showed that RGD-GEM-LPs uptake was approximately 2.5-fold higher than that of GEM-LPs, which was attributed to the targeting capacity of αvβ3 integrin.

Ji et al. [48] synthesized a matrix metalloproteinase-2 (MMP-2) responsive peptide (SDK(C18)SGPLG-IAGQSK(C18)DS)-hybrid liposome loaded with pirfenidone (MRPL-PFD) to treat pancreatic cancer. Pancreatic tumor development involves the proliferation of pancreatic stellate cells (PSCs) and secretion of ECM in the tumor stroma, which reduces drug delivery and penetration in tumor tissue. Therefore, decreasing ECM secretions through the regulation of PSCs has the ability to enhance the penetration of therapeutic drugs, thus enhancing their therapeutic efficacy. The developed MRPL-PFDs were explicitly designed to release PFD at the pancreatic tumor site leading to the downregulation of the ECM by the PSCs; hence, enabling the penetration of GEM into the tumor tissue.

Carbohydrates

Glycosylation refers to the reaction in which a carbohydrate is attached to a functional group of another molecule. Abnormal glycosylation and carbohydrate alterations on cell membranes are associated with various cancer processes, including tumorigenesis, malignant transformation, and tumor metastasis [49]. To be recognized and taken up by cells, carbohydrate-decorated liposomes require suitable receptors. Lectins are a class of carbohydrate-binding proteins that are highly specific for certain sugar groups [50]. Lectins are overexpressed on several cell surfaces; hence glycosylated vehicles can be recognized and endocytosed by lectin receptors [51]. Several liposome preparations displaying various carbohydrates on the outer membrane surface of liposomes have been reported in literature.

Xiong et al. [52] synthesized mannosylated paclitaxel (PTX)-containing liposomes targeting the mannose receptor (MR) in the colon cancer (CT26) cell line. *In vitro* and *in vivo* studies showed that mannosylated liposomes had higher uptake by CT26 cells, enhanced tumor inhibition rate, and no notable *in vivo* toxicity. Minnelli et al. [53] investigated the therapeutic effect of mannose-6-phosphate (M6P)

liposomes in breast cancer cells (MCF7) and human dermal fibroblast cells (HDF). The liposomes were loaded with the model drug calcein and N-hexanoyl-D-erythro-sphingosine (C6Cer). DLS measurements, spectrophotometric turbidity measurements, and flow cytometry analysis showed increased uptake of M6P liposomes by the MCF7 cells compared to HDF cells. Tian et al. [54] reported a dual-functional hyaluronic acid (HA) modified-PTX loaded liposome system targeting both the CD44 receptor and mitochondria to reduce drug-resistance of cancer cells and trigger apoptosis. The *in vivo* study results showed that the uptake of HA liposomes increased by approximately five-fold in A549/T cells compared with uncoated liposomes.

Dual targeting

A recent trend in the surface functionalization of liposomes involves the decoration of the liposomal surface with two ligands. Dual-targeted liposomes offer several advantages, such as; targeting two or more receptors, subsequently delivering more drugs to the cells. Another advantage is enabling the loaded drug to exert therapeutic effects in multiple ways. Dual-targeting could also be a strategy to reduce normal tissue toxicity [55,56]. Several research groups have developed dual-ligand liposome formulations. For example, Ke et al. [57] synthesized aspartate (Asp_8) and folate modified DOX-loaded liposomes (A/F-LS). Characterization tests showed that the %EE of DOX for all liposomes was more than 90 %, and the surface modification did not affect the ultimate %EE. The *in vitro* assays and *in vivo* distribution imaging indicated that A/F-LS has a strong bond targeting effect. A/F-LS showed high cellular uptake by FR-rich tumor cells, which resulted in the high cytotoxicity of the encapsulated DOX. In addition, pharmacokinetics and tissue distribution studies suggested that the developed liposomes had prolonged blood circulation times and favored DOX accumulation in the tumor. Lakkadwala et al. [58] obtained similar results in another study involving dual-targeting liposomes. These liposomes were functionalized with Tf and a cell-penetrating peptide (CPP). The *in vitro* and *in vivo* studies results showed that Tf-CPP liposomes resulted in a more than 10-fold increase in DOX accumulation and approximately a three-fold increase in erlotinib accumulation in mice brains, respectively.

Pu et al. [59] designed and developed two types of dual-functionalized triple-negative breast cancer targeting (TNBC) liposomes. The developed liposomes were modified with a fructose and RGD peptide (Fru-RGD-Lip) to actively recognize the fructose transporter $GLUT_5$ and the integrin $\alpha_v\beta_3$. The results indicated that the PXT-loaded Fru-RGD-Lip achieved the greatest growth inhibition of MDA-MB-231 and 4T1 cells. Table 1 provides further examples of recent studies focusing on dual functionalization.

Stimuli-responsive Liposomes

The tumor microenvironment has certain defining characteristics (e.g., lower pH, higher temperature, and enzymatic level) that can be exploited to enhance liposomal release at target sites. Stimuli-

responsive liposomes are designed to become destabilized and release their payload upon exposure to a specific stimulus. Stimuli are broadly divided into internal and external triggers. Internal triggers include pH, temperature, redox, and enzyme level, whereas external triggers include temperature, magnetic field, ultrasound (US), and light [8,60].

pH-responsive Liposomes

Aerobic glycolysis (the Warburg effect), one of the hallmarks of cancer, states that tumors exhibit increased glucose uptake and lactic acid production, even in the presence of oxygen [61]. This increased acid production leads to lower pH levels in cancer cells (pH range of 4.8-6.5) [62]. Therefore, pH-responsive liposomes are designed to securely store anti-cancer drugs at physiological pH (~7.4), but rapidly release the drug below a pH trigger point [60,63].

Vila-Caballer et al. [64] developed PEGylated pH-responsive liposomes for the delivery of bovine serum albumin (BSA) to the bladder epithelium. The liposomes were prepared using $mPEG_{5kDa}$-DSPE and stearoyl-PEG-poly(methacryloyl sulfadimethoxine) (stearoyl-PEG-polySDM). Confocal microscopy and cytofluorimetry results showed that at pH 7.4, the internalization of BSA-loaded liposomes by MB49 (mouse bladder carcinoma cells) was remarkably lower than that measured at pH 6.5. Also, control liposomes at pH 7.4 and 6.5 did not deliver BSA to the bladder epithelium, *in vivo*. In contrast, the pH-sensitive liposomes efficiently delivered BSA to MB49 cells at the lower investigated pH. Zhai et al. [65] coupled the polypeptide DVar7 with DSPE-PEG_{2000}-MAL to form DSPE-PEG_{2000}-DVar7. DVar7 is a member of the pH-Low Insertion Peptides (pHLIPS) family, which can target the acidic microenvironment of the tumor. The synthesized liposomes were loaded with DOX, then characterized using dynamic light scattering (DLS), ultraviolet (UV) spectrophotometer and electron microscopy. Following characterization, the acidic-specific uptake of liposomes by tumor cells was investigated using breast cancer (MDA-MB-435S) cells. The prepared pH-sensitive DOX-loaded liposomes had an average particle size of around 130 nm, high encapsulation efficiency (~98 %) and good stability *in vitro*. In addition, the *in vivo* studies showed that the pH-responsive liposomes had the best tumor suppression.

Redox-responsive Liposomes

Another feature of tumors is a reducing microenvironment strictly controlled by the reduction and oxidation states of $NADPH/NADP^+$ and glutathione (GSH, GSH/GSSG) [60,66,67]. The intracellular concentration of GSH in tumors can reach ten mM, while the extracellular concentration ranges between 2 and 20 μM [66]. Redox sensitivity offers several advantages as a triggering mechanism: first, redox-responsive liposomes are stable in healthy tissues, reducing the toxicity and side effects of both the carrier and payload. Second, they are highly attuned to high GSH concentrations in tumor cells. Finally, the cytoplasm release is theorized to have better therapeutic effects than other locations in the cell [66,68].

Wang et al. [69] developed redox-responsive liposomes based on a disulfide-derivative paclitaxel-ss-lysophosphatidylcholine prodrug (PTX-ss-PC). The developed liposomes dissociated rapidly in a reduction medium. Additionally, the *in vitro* cytotoxicity of the liposomes was measured against breast and lung cancer cells. The results showed that the PTX-ss-PC liposomes demonstrated promising GSH-mediated tumor growth inhibition activity. Another study investigating PTX-ss-PC liposomes was conducted by Du et al. [70]. PTX/SS-LPs were characterized using DLS and TEM. The results of the characterization tests revealed unilamellar vesicles with an average size of 108.6 ± 2.4 nm. The redox-sensitivity of PTX/SS-LPs was confirmed by the changes in the size, morphology, as well as the rapid release of PTX upon the addition of dithiothreitol (DTT). The final release rates indicated that PTX/SS-LPs were responsive to reductive environments. The *in vitro* studies in MCF-7 and A549 cells showed increased cytotoxicity in the cells treated with PTX/SS-LPs compared to cells treated with control liposomes. *In vivo* studies were conducted using BALB/c mice; after three weeks, the tumor volumes of the groups treated with PTX/SS-LP, PTX/LP were at least three-fold lower compared to the control group.

Enzyme-responsive Liposomes

Pathological conditions, such as infection, inflammation, and cancer, lead to an increase in the concentrations of several enzymes at the diseased site. This abnormality can be used to trigger structural changes in enzyme-sensitive liposomes leading to the release of the encapsulated payload [71,72]. Shchegravina et al. [73] reported phospholipase A_2-responsive liposomes incorporating colchicinoid lipid prodrugs in their lipid bilayer. Upon exposure to elevated levels of phospholipase A_2, especially $sPLA_2$ analog, the liposomes released colchicinoid-containing fatty acids, which underwent further hydrolysis by non-specific esterases and released the active species. Ji et al. [74] developed β-cyclodextrin (βCD) modified MMP-2 responsive liposomes, integrating antifibrosis PFD and the chemotherapeutic drug GEM for the treatment of pancreatic cancer; the developed system was named LRC-GEM-PFD. The drug release profiles showed that LRC-GEMs released around three fourth of the loaded agent after two days of the MMP-2 treatment. The tumor penetration of the developed system *in vivo* was determined by labeling the liposomes with rhodamine (Rhd). Mice xenografted with PSCs/Panc-1 cancer cells were intravenously injected with LRC, free PFD, and LRC-PFD. The average penetration depth of Rhd in each group was, 967.8 ± 56.3 μm, 337.8 ± 32.3 μm and 161.4 ± 16.1 μm for the LRC-PFD, free PFD, and LRC groups, respectively.

Pourhassan et al. [75] evaluated the antiproliferative capacity of oxaliplatin (L-OHP) encapsulated in $sPLA_2$ sensitive liposomes in human colon carcinoma (HT-29and Colo205) cell lines. In both tested cell lines, liposomal L-OHP was highly cytotoxic, inhibiting cell growth by 50 %. The results of the *in vivo* studies showed that the $sPLA_2$-sensitive liposomal formulations did not significantly improve the anti-tumor effect of L-OHP compared to control liposomes. The liposomal formulations demonstrated a minor

increase in growth-rate inhibition relative to the free drug; however, all of the tested formulations exhibited around 45 % treatment-to-control ratios (%T/C) and were therefore statistically insignificant.

Temperature-responsive Liposomes

Inflammation sites and tumors are characterized by elevated temperatures relative to healthy tissues. Hyperthermia can induce increased tumor tissue permeability, which can lead to enhanced liposome uptake and drug delivery. Release from thermosensitive liposomes can be triggered either through the elevated temperatures which are characteristic of tumors or by externally manipulating the temperature. Thermo-sensitive liposomes are designed to release their contents at elevated temperatures (around 40-45°C) through disruption of the orderly packing of the lipids in the bilayer.

The most commonly used thermo-sensitive lipid is dipalmitoylphosphatidylcholine (DPPC), an example of a commercially available thermosensitive liposomes (TSLs) include Thermodox® (Celsion, Lawrenceville, NJ, USA) [76–78]. Several research groups have investigated the use of thermosensitive liposomes in cancer therapy. Motamarry et al. [79] used real-time fluorescence imaging to visualize the uptake of thermosensitive liposomal DOX (Thermodox ®). Nude mice bearing Lewis lung carcinoma cells were injected with Theromodox®, and localized hyperthermia was induced by superficially heating the tumors using a probe. *In vivo* fluorescence imaging was performed before, during, and 5 min following heating. After imaging, the tumors were excised, and the drug uptake was quantified using high-performance liquid chromatography (HPLC). The imaging results showed that the fluorescence of heated tumors increased by four-fold (after 15 min of heating), nine-fold (after 30 min of heating), and thirteen-fold (after 60 min of heating) compared to the unheated control tumors. In another study involving Thermodox, Derieppe et al. [80] used fibered confocal fluorescence microscopy (FCFM) to monitor the penetration of released-DOX in a subcutaneous rat R1 rhabdomyosarcoma xenograft model. The TSLs were injected intravenously then the tumor-bearing leg was immersed in a water bath preheated to 43°C. The real-time FCFM of released-DOX penetration demonstrated an increased fluorescence signal in tumor cell nuclei, indicating an increasing DOX concentration upon cell uptake.

Lyu et al. [81] prepared TSLs to deliver an MMP inhibitor, marimastat (MATT), to the tumor microenvironment. The results of *in vitro* and *in vivo* studies revealed that TSLs rapidly released their payloads at 42°C and achieved a twenty-fold decrease in tumor growth in mammary carcinoma (4T1) tumor-bearing mice. Furthermore, the developed liposomes reduced MMP-2 and MMP-9 expression *in vivo* and causing a 7-fold decrease in metastatic lung nodules.

Light-responsive Liposomes

Light-triggered delivery systems are dependent on the penetration depth of the selected light source, and the photosensitizing properties of the therapeutic agents [67]. Different light wavelengths have been

reported as triggers for drug release, including visible, UV, and near-infrared (NIR). The wavelengths preferred in biomedical applications are in the NIR regions (~700 nm to 1100 nm) because at this wavelength, the light penetration is more than 1 cm [60].

Chen et al. [82] designed a NIR responsive bubble-generating thermosensitive liposome (BTSL) system entrapping the reactive carbocyanine dye (Cypate), DOX, and NH_4HCO_3. Cypate is a NIR fluorescent dye with an absorbance maximum at 778 nm and an emission maximum at 805 nm with a high extinction coefficient of 224,000 $(mol/L)^{-1}cm^{-1}$. *In vitro* release studies showed that the amount of DOX released from BTSL was higher than that of $(NH_4)_2SO_4$ liposomes at 42°C. The NIR irradiation caused an increase in temperature, which led to the decomposition of NH_4HCO_3 and the subsequent generation of a large number of carbon dioxide bubbles, the rise in temperature, in turn, caused the rapid release of drugs from BTSLs.

To address hypoxia-associated photodynamic resistance, an issue commonly encountered in the photodynamic therapy of tumors, Yu et al. [83] developed oxygen self-sufficient liposomes containing aza-BODIPY dye (B1), Calcium peroxide (CaO_2) NPs in the hydrophobic layer and NH_4HCO_3 in the hydrophilic cavity (denoted as CaO_2/B1/NH_4HCO_3 lipo). Upon exposure to NIR irradiation, two-photon absorption activated B1 inducing hyperthermia, which further triggered the decomposition of NH_4HCO_3 into NH_3, H_2O, and CO_2. Subsequently, CO_2 reacted with CaO_2 to rapidly and self-sufficiently generate oxygen. The developed liposomal system presented a valuable approach to regulating intra-tumoral hypoxia and overcoming hypoxia-associated photodynamic therapy resistance.

Magnetic-responsive Liposomes

Magnetic resonance imaging (MRI) is a well-established imaging technique; however, magnetic fields are being used in other biomedical applications, such as controlling drug release from magnetic-field responsive carriers [60]. Magnetic nanoparticles (MNPs) are one of the promising carriers for magnetic field responsive targeted delivery due to their biocompatibility and unique features [84]. Magnetic stimulation can cause release either through localized hyperthermia or through magnetic-field drug targeting [60]. Combining MNPs and liposomes was first introduced in 1988 by Marcel De Cuyper and Marcel Joniau [85]. Ever since, these “magnetoliposomes” have been used in MRI imaging, targeted drug delivery, and hyperthermia-mediated controlled drug release [67]. The most commonly used MNPs in targeted delivery are superparamagnetic iron oxide nanoparticles (SPIONs). Several studies have investigated the use of magnetoliposomes in targeted cancer therapy.

Hardiansyah et al. [86] investigated the therapeutic efficacy of DOX-loaded PEGylated magnetic liposomes. The prepared magnetoliposomes exhibited inductive heating from 37°C to 56 °C utilizing high-frequency magnetic fields (HFMF). The cytotoxicity studies were conducted using L-929 fibroblasts and

HeLa cells. The results of the assay showed that PEGylated magnetic liposomes had no cytotoxicity effects against fibroblast L-929 cells. In contrast, the cytotoxicity of the released DOX to HeLa cells was a function of DOX concentration. Lu et al. [87] synthesized TSLs co-encapsulating MNPs and Camptosar (CPT-11). This formulation was designed to release its contents upon exposure to a high frequency alternating magnetic field (AMF). *In vitro* studies showed that increasing the temperature to 43°C caused a burst release of CPT-11 from the magnetoliposomes; in addition, the induced magnetic thermal effects lead to a drug release plateau of 97%, in contrast to the 19 % release obtained in the absence of AMF.

Ultrasound (US)-responsive Liposomes

US-mediated drug release from liposomes involves the disruption of the liposomal membrane and occurs in response to either a rise in temperature or the mechanical effects produced by US. With regard to the thermal effects of US, liposomes are stable in the physiological temperature range; however, upon exposure to US, the temperature rises in that area, which disrupts the lipid bilayer, causing the liposomes to release their contents [88,89]. Moreover, thermal effects can alter vascular permeability, enhancing the uptake of liposomes. The mechanical effects of US are manifested in the form of acoustic cavitation and sonoporation.

Acoustic cavitation refers to the growth and collapse of microbubbles due to an oscillating pressure field in liquids [90]. Sonoporation is the use of sound waves, typically at ultrasonic frequencies, to produce acoustic cavitation to enhance the permeability of the cell plasma membrane [91]. Acoustic cavitation is categorized into stable and transient cavitation, both of which are capable of inducing sonoporation. Stable cavitation can create pores by high shear stresses caused by microstreaming around oscillating bubbles, whereas inertial cavitation creates pores by penetration of liquid jets formed by the asymmetric collapse of bubbles near surfaces [92]. According to literature, the effect of transient cavitation on drug release is more substantial than stable cavitation because transient cavitation can induce additional mechanical effects such as shockwaves and micro-jets that complement the effects of sonoporation [88,89,93,94].

Xin et al. [95] prepared liposomes encapsulating Mitoxantrone (MXT) and PLGA NPs. In their study, the PLGA NPs were used as US-responsive agents instead of conventional microbubbles. The release of MXT-entrapped liposomes was investigated *in vitro* and *in vivo*. The cumulative drug release of PLGA NPs encapsulating liposomes was higher than fifty percent after the application of US, while this value was around 9 percent without US stimulation. Santos et al. [96] developed a system integrating focused US (FUS) with two-photon microscopy (2PM) for the real-time imaging of DOX release from Thermodox® during FUS- induced hyperthermia *in vivo*. The *in vivo* studies were conducted using a DSWC murine tumor model, and findings indicated that ten-30 s bursts of FUS hyperthermia to 42°C were able to achieve almost

half of the interstitial drug concentration that was observed with a continuous 20 min sonication, which corresponded to an almost 6-fold longer integrated exposure time.

Dual and Multi-stimuli Responsive Liposomes

A recent advancement in stimuli-responsive drug delivery is the development of dual or multi-stimuli responsive liposomes. These triggers can be endogenous, exogenous, or a combination of both. Xing et al. [97] combined light and temperature triggering to release the contents of their liposomes. The authors synthesized liposomes encapsulating gold nanoparticles (Au NPs) and DOX (Au/DOX-lip). The Au/DOX-liposomes were irradiated with a NIR light, which lead to the release of the Au NPs. The Au NPs then penetrated deeper into the tumor tissue; simultaneously, the hyperthermia induced by the irradiation increased the membrane permeability of both the tumor cells and liposomes, facilitating the release and accumulation of DOX in tumor cells. The developed system showed significant anti-tumor effects, with a tumor growth inhibition rate of around seventy-eight percent.

In another study, Chen et al. [98] developed pH-sensitive NIR-responsive liposomes coated with pH-sensitive poly(methacryloyl sulfadimethoxine) (PSD) and encapsulating Cypate, DOX, and NH_4HCO_3 (PSD/DOX/Cypate-BTSL). In a mouse breast (4T1) tumor model, the developed system enhanced cellular uptake and cytotoxicity at a pH of 6.5 when stimulated by NIR irradiation. *In vivo* results suggested that releasing liposomal contents using NIR can enhance DOX accumulation at the tumor site, anti-tumor efficacy and reduce the systemic side effects of DOX. Wang et al. [99] synthesized gold nanoshells coated chitosan liposomes loaded with Res (GNS-CTS-Res-lips). Res release was triggered using pH and NIR light. First, the pH-mediated release was tested and showed around fifty-seven percent release of Res at pH 5.0 (compared to a release of twenty percent at pH 7.4). Next, the drug release changes in response to NIR light pulses were investigated; the GNS-CTS-Res-lips were irradiated with NIR at 5-min intervals (at both pH 5.0 and 7.4). Without NIR irradiation, the release was slow, and plateaued at about 6 percent (pH 7.4) and fourteen percent (pH 5.0); however, upon exposure to NIR, the release rate increased to around forty percent at pH 7.4 and approximately eighty percent at pH 5.0.

Shaghasemi et al. [100] loaded small unilamellar liposomes with SPIONs and the model drug calcein. The authors hypothesized that the release mechanism involved the local heating of the embedded SPION through Néel relaxation in an AMF. The release results showed that the concentration of SPIONs in the membrane is a determining factor for calcein release from liposomes when exposed to an AMF. At a two wt% SPION concentration, only twenty-eight percent of calcein was released after the first pulse (duration of 2 min), and forty-four percent after 5 pulses. When the concentration was increased to four wt% SPION, the first 2-min pulses released around forty-eight percent of the payload. Moreover, only three pulses were

required to reach maximum release of calcein, which was approximately ninety percent. Table 2 presents a summary of some other relevant studies.

Combining Surface Functionalization and Stimuli-mediated Release from Liposomes

The development of stimuli-responsive liposomes modified with different moieties to target receptors overexpressed on cancer cells, or the tumor microenvironment is a recent and promising approach to maximize the benefits of targeted cancer therapy. Lee et al. [101] synthesized HA grafted DTX loaded pH-responsive liposomes. Functional 3-diethylaminopropyl (DEAP) groups were used to make a pH-responsive polymer; three liposomal formulations with three different molar ratios of DEAP to HA were prepared, namely, HA-g-$DEAP_{0.15}$, HA-g-$DEAP_{0.25}$, and HA-g-$DEAP_{0.40}$. Out of the three formulations, HA-g-$DEAP_{0.40}$ gave the best results in terms of release of the encapsulated DTX in response to pH reduction to endosomal pH (i.e., 6.5). Moreover, HA liposomes were effective at entering the human colon carcinoma (HCT-116) cells with a CD44 receptor overexpression causing a significant increase in HCT-116 tumor cell death.

Yang et al. [102] developed Asparagine-Glycine-Arginine (NGR) peptide modified thermosensitive liposomes containing a reducible siRNA-CPPs for tumor-specific siRNA transfection (siRNA-CPPs/NGR-TSL). The developed liposomal system had a particle size of about 90 nm, and a %EE of approximately 86 %. In the *in vitro* studies, both the preheated free siRNA-CPPs and siRNA-CPPs/NGR-TSL silenced c-myc regulator gene in human fibrosarcoma (HT-1080) cells; however, when tested *in vivo*, siRNA-CPPs/NGR-TSL displayed about 3-fold better anti-tumor efficacy and around 2-fold superior gene silencing efficiency compared with free siRNA-CPPs under hyperthermia. Table 3 presents a summary of some recently published studies focused on the use of surface functionalization and stimuli responsiveness in a single liposomal formulation for the efficient delivery of anti-cancer therapeutics.

Future Prospects

Despite the reported preclinical successes of liposomal drug delivery systems, their real impact in cancer therapy remains limited. This is often attributed to the fact that the field is a relatively new area of science [103]. Many studies have suggested that this attenuated therapeutic efficacy is mainly due to formulation design, and tumor pathophysiology [104,105].

As mentioned earlier, the development and success of nanomedicine can be ascribed to the discovery of the EPR effect. However, inter- and intra-tumoral variability, as well as tumor variability as a

function of cancer type, and among patients has been shown to limit the efficacy of the EPR effect, foster drug resistance, and complicate the selection of globally effective therapeutic agents [106,107].

Some of the methods proposed to address tumor heterogeneity and its implications on liposomal anti-cancer drug delivery include the modulation of tumor vasculature by increasing the blood pressure of a patient [104,108]. For example, hypertension caused by the systemic administration of angiotensin-II (AT-II) leads to the passive opening of pores in the tumor endothelium, which may improve the delivery of liposomes to tumor sites [109]. Increasing vascular permeability using nitric oxide (NO)-releasing/inducing agents (e.g., nitroglycerin) can also contribute to augmenting the EPR effect. These agents liberate nitrite, which is converted to NO under the hypoxic conditions of tumor tissues. Administration of NO-releasing agents should thus release NO and enhance the EPR effect by inducing vasodilation [104,109]. Moreover, simultaneously targeting the vascular, tissue, and cellular levels have been suggested as a viable approach to enhance the EPR effect and overcome cancer MDR. Multi-tier targeting can be achieved using more than one anti-neoplastic agent, and liposomes have shown effective co-loading and a sustained release of several anti-cancer agents [104,108]. However, a commonly encountered issue with the co-loading of liposomes is the low water-solubility of one or both anti-cancer medications, which can lead to reduced liposomal loading capacity and poor stability.

Although the active drug loading method effectively uses the electrostatic gradient across the lipid bilayer as a driving force to load drugs into liposomes, this method is more applicable to amphiphilic soluble drugs. Solvent-assisted active loading technology (SALT) is an advancement of the active loading method to improve encapsulation efficiency and formulation stability. [110,111].

In addition to targeting pathways and modifications commonly implicated in MDR, the characteristics of the tumor could be used to design personalized treatment options. Biomarkers such as tumor-specific protein overexpression and mutations in driver genes are currently used to predict tumor response to selective targeted therapies, with additional biomarkers rapidly emerging. Therefore, biomarker-specific treatment plans can be tailored to each patient according to their tumor molecular profile [112,113]. For example, the I-PREDICT study involved customized therapies based on molecular profiling of cancer patients [114]. The underlying hypothesis is that targeting only one molecular alteration of a tumor is often insufficient to yield improved disease control rates. Moreover, so far, precision medicine oncology trials have been focused on molecular matching with predetermined monotherapies. However, several trials exhibited low matching rates, often in the range of 5–10% [112,113]. A recent study took into account several actionable molecular alterations and proposed customized multidrug regimens to achieve durable anti-tumor activity [114].

Another emerging innovation in precision medicine is the testing of circulating tumor-specific biomarkers, including circulating tumor cells (CTC), circulating tumor DNA (ctDNA), as well as RNAs,

proteins, or metabolites that are present in body fluids [112,115]. Liquid biopsies are minimally invasive procedures that can provide a dynamic assessment of tumors and predictive biomarkers [116].

Another promising aspect of precision medicine is personalized dosing regimens tailored to patients' tumor profile, and drug penetration in tumor tissue [117,118]. Before treatment, non-invasive imaging techniques using drug model dyes or radiolabeled drugs can be used to assess the heterogeneity of the tumor and detect the presence of the target at the tumor site. Moreover, assessment of the tumor microenvironment (e.g., vascular and lymphatic architecture and hypoxia) may provide information useful in drug selection and predicting drug behavior [117]. During treatment, plasma pharmacokinetic (PK) sampling can be used to ensure optimal bioavailability in the blood and achieve the maximal binding capacity in tumor tissues [119]. Along the course of the treatment, tumor tissue biopsies can be used to determine drug penetration at a microscopic level; while imaging can be used to monitor drug response and/or drug resistance. Several conventional imaging modalities (e.g., CT, PET, SPECT, and MRI) have been applied, while several novel imaging techniques (e.g., dual-energy CT, diffusion-weighted MRI, and bioluminescence imaging) are being investigated for such applications [120,121]. The gathered information can then be integrated with preclinical and prior knowledge using mathematical models and computer simulations to decide on the dosing regimen and further adapt the treatment plan [117].

Other strategies to overcome MDR and enhance the multiple delivery of chemotherapeutics to cancer cells include the use of external stimuli. US is of special interest because it is non-invasive, can be controlled both spatially and temporally, and can penetrate deep into the body. Moreover, several studies have shown that it can increase the permeability of blood vessels and cell membranes [122,123]. Given the promise of US as a triggering mechanism, a great deal of focus has been placed on the optimization of US exposure parameters (i.e. frequency, intensity, negative pressure, duration, and duty cycle).

Some studies have reported that beyond the minimum pressure threshold, US-induced release increases linearly with increasing peak negative pressure [123]. Other studies focused on establishing the role of inertial cavitation in drug release reported a linear relationship between drug release and acoustic amplitude [124–126]. Moreover, drug release was shown to increase with increasing US exposure time [123,127]. This is often attributed to sonoporation (pore formation due to acoustic cavitation), and the self-sealing properties of lipid membranes. Some reports suggested that lipid membranes reseal rapidly after sonoporation; however, when exposed to longer pulses, liposomes require more time to resume their formation [128]. Despite the amount of research US-mediated liposomal release, there is still a need for further research into the optimization of US parameters to allow this technology to transition to clinical settings.

Another object of intense research is gene delivery for cancer therapy. Different approaches have been investigated for cancer gene therapy; these include induction of apoptosis, immune modulation,

correction of gene defects, inhibition of tumor invasion, and gene therapy to improve chemo- and radiotherapy [129].

The main obstacle in gene therapy is to ensure that enough genetic material is being delivered into the target cells and to maintain gene expression for the desired period [129,130]. The genetic material can be introduced using different modalities, which can be broadly grouped into physical, viral, non-viral, and bacterial or yeast deliveries. Currently, viral vectors are considered the most effective of all gene delivery methods for *in vivo* gene transfer, with the most commonly used viruses including adenoviruses, lentiviruses and retroviruses [129–131]. The biological properties of viruses are what made them appealing as vectors for gene delivery; however, their immunogenicity, limited genetic-load, and cancer risk due to the mutagenicity of viruses led to the development of non-viral vectors supported by nanotechnology [130,132]. The low immunogenicity and easy penetration of the cell membranes made lipid-based NPs and exosomes two of the most promising carriers for gene delivery. A number of NP-based gene delivery systems have reached clinical trials, most of which involved a cationic polymer for binding nucleic acids, a PEG steric stabilization agent, and a targeting ligand for binding to receptors on target cells. However, to date, none of these NP-based gene therapeutics have been approved by the FDA [132,133].

Another exciting aspect of gene therapy is immunotherapy. Since most tumor cells have the ability to go undetected by the immune system, immune gene therapy involves the transfer of exogenous immune system-related genes, such as cytokines and receptors, tumor antigens, and costimulatory molecules, into appropriate target cells, thus improving the anti-tumor immunity of the human body. Currently, the most commonly used immune gene therapy approaches are cytokine gene therapy, tumor vaccine therapy, and introducing chimeric antigen receptor (CAR) to T-cells (CAR-T) [134]. Amongst the different immune gene therapy methods, cancer vaccines have experienced slower growth and encountered more challenges.

Underwhelming initial results have led to clinical trials aimed at increasing tumor antigenicity in order to enhance the immune-mediated tumor lysis by T-cells [130,131]. One such approach involves genetically modified antigen-presenting cells (i.e., dendritic cells, macrophages, and activated B-cells), with dendritic cells being the most robust antigen-presenting cells in the human body. After tumor cells and immature DCs are isolated from the patient, and specific antigens of tumor cells are identified, the vaccine can be prepared by transfecting tumor antigen-encoded genes into DCs. The particular antigen can then be processed and expressed continuously in DCs, such that when the DCs are injected back into the patient, they would activate the related T-cells and induce a specific anti-tumor immune response [134].

Another proposed approach comprises DNA plasmids containing a genetic sequence that encodes a desired antigen with other transcriptional elements to be used as a cancer vaccine. This technique is easy to develop and produce commercially and is considered relatively safer than viral or bacterial vectors

because it does not cause infection or autoimmune disorders. However, the effectiveness of these vaccines fades with time, giving rise for frequent booster immunizations [130].

In the future, the advancements and increased use of genomic analyses, progress achieved in the development of safe and effective vectors for gene transfer, as well as the assessment of host humoral and cellular immunity, will facilitate the selection of the most appropriate gene therapy for each patient. This will revolutionize cancer therapy, from a 'one-size-fits-all' treatment strategy to more individualized cancer treatments tailored to fit the patient's specific genomic constituents, host immune status, and cancer genetic profile. Such therapies are expected to be fast, effective, relatively less toxic, inexpensive, with higher cure rates.

Conclusion

Encapsulating anti-cancer therapeutics in nanocarriers has proven to be a promising alternative to the conventional cancer treatment methods, as it improves both the safety and efficacy of anti-cancer therapeutics. Several liposome formulations are commercially available in the market, e.g., Doxil®, DaunoXome®, and Depocyt®. Surface functionalization and various stimuli have been introduced to overcome the limitations of conventional liposomes and further enhance their therapeutic efficacy. This review highlighted some of the recent advances in surface functionalization and optimization of liposomes to allow the delivery of chemotherapeutics locally upon internal and/or external stimulation. In addition, we presented an overview of relevant *in vitro* and *in vivo* studies pertaining to ligand-targeted and stimuli-responsive liposomes.

AUTHOR INFORMATION

Corresponding Author

*E-mail: ghusseini@aus.edu.

ORCID

Ghaleb A. Husseini: 0000-0002-7244-3105

Author Contributions

The manuscript was written through the contributions of all authors. All authors have given approval to the final version of the manuscript.

Notes

The authors declare no competing financial interest.

Acknowledgements:

The authors would like to acknowledge the financial support of the American University of Sharjah Faculty

Research Grants (FRGs and eFRGs), the Al-Jalila Foundation (AJF 2015555), the Al Qasimi Foundation, the Patient's Friends Committee-Sharjah, the Biosciences and Bioengineering Research Institute (BBRI18-CEN-11), and the Dana Gas Endowed Chair for Chemical Engineering.

References

(1) World Health Organization. Noncommunicable diseases https://www.who.int/news-room/fact-sheets/detail/noncommunicable-diseases (accessed Mar 8, 2020).

(2) American Cancer Society. *Cancer Facts and Figures 2021*; Atlanta, 2021.

(3) Morales-Cruz, M.; Delgado, Y.; Castillo, B.; Figueroa, C. M.; Molina, A. M.; Torres, A.; Milián, M.; Griebenow, K. Smart Targeting to Improve Cancer Therapeutics. *Drug Design, Development and Therapy*. Dove Medical Press Ltd. 2019, pp 3753–3772. https://doi.org/10.2147/DDDT.S219489.

(4) Yildizhan, H.; Barkan, N. P.; Karahisar Turan, S.; Demiralp, Ö.; Özel Demiralp, F. D.; Uslu, B.; Özkan, S. A. Treatment Strategies in Cancer from Past to Present. In *Drug Targeting and Stimuli Sensitive Drug Delivery Systems*; Elsevier, 2018; pp 1–37. https://doi.org/10.1016/b978-0-12-813689-8.00001-x.

(5) National Cancer Institute. Types of Cancer Treatment https://www.cancer.gov/about-cancer/treatment/types (accessed Mar 9, 2020).

(6) Pucci, C.; Martinelli, C.; Ciofani, G. Innovative Approaches for Cancer Treatment: Current Perspectives and New Challenges. *ecancermedicalscience*. ecancer Global Foundation September 10, 2019. https://doi.org/10.3332/ecancer.2019.961.

(7) Charmsaz, S.; Prencipe, M.; Kiely, M.; Pidgeon, G. P.; Collins, D. M. Innovative Technologies Changing Cancer Treatment. *Cancers (Basel).* **2018**, *10* (6). https://doi.org/10.3390/cancers10060208.

(8) Hossen, S.; Hossain, M. K.; Basher, M. K.; Mia, M. N. H.; Rahman, M. T.; Uddin, M. J. Smart Nanocarrier-Based Drug Delivery Systems for Cancer Therapy and Toxicity Studies: A Review. *Journal of Advanced Research*. Elsevier B.V. January 1, 2019, pp 1–18. https://doi.org/10.1016/j.jare.2018.06.005.

(9) Kalaydina, R. V.; Bajwa, K.; Qorri, B.; Decarlo, A.; Szewczuk, M. R. Recent Advances in "Smart" Delivery Systems for Extended Drug Release in Cancer Therapy. *Int. J. Nanomedicine* **2018**, *13*, 4727–4745. https://doi.org/10.2147/IJN.S168053.

(10) Toy, R.; Peiris, P. M.; Ghaghada, K. B.; Karathanasis, E. Shaping Cancer Nanomedicine: The Effect of Particle Shape on the in Vivo Journey of Nanoparticles. *Nanomedicine*. Future Medicine Ltd. 2014, pp 121–134. https://doi.org/10.2217/nnm.13.191.

(11) Steichen, S. D.; Caldorera-Moore, M.; Peppas, N. A. A Review of Current Nanoparticle and Targeting Moieties for the Delivery of Cancer Therapeutics. *Eur. J. Pharm. Sci.* **2013**, *48* (3), 416–427. https://doi.org/10.1016/j.ejps.2012.12.006.

(12) Taurin, S.; Nehoff, H.; Van Aswegen, T.; Greish, K. Tumor Vasculature, EPR Effect, and Anticancer Nanomedicine: Connecting the Dots. In *Cancer Targeted Drug Delivery: An Elusive Dream*; Bae, Y. H., Mrsny, R. J., Park, K., Eds.; New York, NY: Springer, 2013; pp 207–239.

https://doi.org/10.1007/978-1-4614-7876-8-8.

(13) Greish, K. Enhanced Permeability and Retention Effect for Selective Targeting of Anticancer Nanomedicine: Are We There Yet? *Drug Discovery Today: Technologies*. Elsevier Ltd June 1, 2012, pp e161–e166. https://doi.org/10.1016/j.ddtec.2011.11.010.

(14) Weissig, V. Liposomes Came First: The Early History of Liposomology. In *Methods in Molecular Biology*; Humana Press Inc., 2017; Vol. 1522, pp 1–15. https://doi.org/10.1007/978-1-4939-6591-5_1.

(15) Olusanya, T. O. B.; Ahmad, R. R. H.; Ibegbu, D. M.; Smith, J. R.; Elkordy, A. A. Liposomal Drug Delivery Systems and Anticancer Drugs. *Molecules* **2018**, *23* (4). https://doi.org/10.3390/molecules23040907.

(16) Akbarzadeh, A.; Rezaei-sadabady, R.; Davaran, S.; Joo, S. W.; Zarghami, N. Liposome: Classification, Preparation, and Applications. *Nanoscale Res. Lett.* **2013**, *8* (1), 102. https://doi.org/10.1186/1556-276X-8-102.

(17) Talegaonkar, S.; Mishra, P.; Khar, R.; Biju, S. Vesicular Systems: An Overview. *Indian J. Pharm. Sci.* **2006**, *68* (2), 141. https://doi.org/10.4103/0250-474x.25707.

(18) Karthikeyan, M.; Balasubramanian, T.; Khaleel, M. I.; Sahl, M.; Rashifa, P. Liposomes: Preparations and Applications. *Int. J. Drug Dev.* **2012**, *4* (4), 108–115.

(19) Riaz, M. K. A.; Riaz, M. K. A.; Zhang, X.; Lin, C.; Wong, K. H.; Chen, X.; Zhang, G.; Lu, A.; Yang, Z. Surface Functionalization and Targeting Strategies of Liposomes in Solid Tumor Therapy: A Review. *Int. J. Mol. Sci.* **2018**, *19* (1). https://doi.org/10.3390/ijms19010195.

(20) Allen, C.; Dos Santos, N.; Gallagher, R.; Chiu, G. N. C.; Shu, Y.; Li, W. M.; Johnstone, S. A.; Janoff, A. S.; Mayer, L. D.; Webb, M. S.; Bally, M. B. Controlling the Physical Behavior and Biological Performance of Liposome Formulations through Use of Surface Grafted Poly(Ethylene Glycol). *Biosci. Rep.* **2002**, *22* (2), 225–250.

(21) Immordino, M. L.; Dosio, F.; Cattel, L. Stealth Liposomes: Review of the Basic Science, Rationale, and Clinical Applications, Existing and Potential. *Int. J. Nanomedicine* **2006**, *1* (3), 297–315.

(22) Jain, A.; Jain, S. K. Advances in Tumor Targeted Liposomes. *Curr. Mol. Med.* **2018**, *18* (1), 44–57. https://doi.org/10.2174/1566524018666180416101522.

(23) Riaz, M. K.; Riaz, M. A.; Zhang, X.; Lin, C.; Wong, K. H.; Chen, X.; Zhang, G.; Lu, A.; Yang, Z. Surface Functionalization and Targeting Strategies of Liposomes in Solid Tumor Therapy: A Review. *Int. J. Mol. Sci.* **2018**, *19* (1). https://doi.org/10.3390/ijms19010195.

(24) Gabizon, A.; Shmeeda, H.; Barenholz, Y. Pharmacokinetics of Pegylated Liposomal Doxorubicin. *Clin. Pharmacokinet.* **2003**, *42* (5), 419–436. https://doi.org/10.2165/00003088-200342050-00002.

(25) Kumar, P.; Huo, P.; Liu, B. Formulation Strategies for Folate-Targeted Liposomes and Their Biomedical Applications. *Pharmaceutics*. MDPI AG August 1, 2019. https://doi.org/10.3390/pharmaceutics11080381.

(26) Moghimipour, E.; Rezaei, M.; Ramezani, Z.; Kouchak, M.; Amini, M.; Angali, K. A.; Dorkoosh, F. A.; Handali, S. Folic Acid-Modified Liposomal Drug Delivery Strategy for Tumor Targeting of 5-Fluorouracil. *Eur. J. Pharm. Sci.* **2018**, *114*, 166–174. https://doi.org/10.1016/j.ejps.2017.12.011.

(27) Zhu, X.; Kong, Y.; Liu, Q.; Lu, Y.; Xing, H.; Lu, X.; Yang, Y.; Xu, J.; Li, N.; Zhao, D.; Chen, X.; Lu, Y. Inhalable Dry Powder Prepared from Folic Acid-Conjugated Docetaxel Liposomes Alters Pharmacodynamic and Pharmacokinetic Properties Relevant to Lung Cancer Chemotherapy. *Pulm. Pharmacol. Ther.* **2019**, *55*, 50–61. https://doi.org/10.1016/j.pupt.2019.02.001.

(28) Wang, W. Y.; Cao, Y. X.; Zhou, X.; Wei, B. Delivery of Folic Acid-Modified Liposomal Curcumin for Targeted Cervical Carcinoma Therapy. *Drug Des. Devel. Ther.* **2019**, *13*, 2205–2213. https://doi.org/10.2147/DDDT.S205787.

(29) Daniels, T. R.; Delgado, T.; Rodriguez, J. A.; Helguera, G.; Penichet, M. L. The Transferrin Receptor Part I: Biology and Targeting with Cytotoxic Antibodies for the Treatment of Cancer. *Clinical Immunology*. Academic Press November 1, 2006, pp 144–158. https://doi.org/10.1016/j.clim.2006.06.010.

(30) Daniels, T. R.; Bernabeu, E.; Rodríguez, J. A.; Patel, S.; Kozman, M.; Chiappetta, D. A.; Holler, E.; Ljubimova, J. Y.; Helguera, G.; Penichet, M. L. The Transferrin Receptor and the Targeted Delivery of Therapeutic Agents against Cancer. *Biochim. Biophys. Acta - Gen. Subj.* **2012**, *1820* (3), 291–317. https://doi.org/10.1016/j.bbagen.2011.07.016.

(31) Joshi, H. A.; Attar, E. S.; Dandekar, P.; Devarajan, P. V. Transferrin Receptor and Targeting Strategies. In *In Targeted Intracellular Drug Delivery by Receptor Mediated Endocytosis*; Springer, Cham, 2019; pp 457–480. https://doi.org/10.1007/978-3-030-29168-6_16.

(32) Jhaveri, A.; Deshpande, P.; Pattni, B.; Torchilin, V. Transferrin-Targeted, Resveratrol-Loaded Liposomes for the Treatment of Glioblastoma. *J. Control. Release* **2018**, *277*, 89–101. https://doi.org/10.1016/J.JCONREL.2018.03.006.

(33) Sakpakdeejaroen, I.; Somani, S.; Laskar, P.; Mullin, M.; Dufès, C. Transferrin-bearing Liposomes Entrapping Plumbagin for Targeted Cancer Therapy. *J. Interdiscip. Nanomedicine* **2019**, *4* (2), 54–71. https://doi.org/10.1002/jin2.56.

(34) Moghimipour, E.; Rezaei, M.; Ramezani, Z.; Kouchak, M.; Amini, M.; Angali, K. A.; Dorkoosh, F. A.; Handali, S. Transferrin Targeted Liposomal 5-Fluorouracil Induced Apoptosis via Mitochondria Signaling Pathway in Cancer Cells. *Life Sci.* **2018**, *194*, 104–110. https://doi.org/10.1016/j.lfs.2017.12.026.

(35) Manjappa, A. S.; Chaudhari, K. R.; Venkataraju, M. P.; Dantuluri, P.; Nanda, B.; Sidda, C.; Sawant, K. K.; Murthy, R. S. R. Antibody Derivatization and Conjugation Strategies: Application in Preparation of Stealth Immunoliposome to Target Chemotherapeutics to Tumor. *J. Control. Release* **2011**, *150* (1), 2–22. https://doi.org/10.1016/j.jconrel.2010.11.002.

(36) Kutova, O. M.; Guryev, E. L.; Sokolova, E. A.; Alzeibak, R.; Balalaeva, I. V. Targeted Delivery to Tumors: Multidirectional Strategies to Improve Treatment Efficiency. *Cancers*. MDPI AG January 1, 2019. https://doi.org/10.3390/cancers11010068.

(37) Eloy, J. O.; Petrilli, R.; Trevizan, L. N. F.; Chorilli, M. Immunoliposomes: A Review on Functionalization Strategies and Targets for Drug Delivery. *Colloids Surfaces B Biointerfaces* **2017**, *159*, 454–467.

(38) Gabbia, D.; Canato, E.; Carraro, V.; Tomasini, L.; Guido, M.; Pasut, G.; De Martin, S. Novel Super Stealth Immunoliposomes for Cancer Targeted Delivery of Doxorubicin: An Innovative Strategy to Reduce Liver Toxicity. *Dig. Liver Dis.* **2019**, *51*, e21. https://doi.org/10.1016/j.dld.2018.11.073.

(39) Khayrani, A. C.; Mahmud, H.; Oo, A. K. K.; Zahra, M. H.; Oze, M.; Du, J.; Alam, M. J.; Afify, S.

M.; Quora, H. A. A.; Shigehiro, T.; Calle, A. S.; Okada, N.; Seno, A.; Fujita, K.; Hamada, H.; Seno, Y.; Mandai, T.; Seno, M. Targeting Ovarian Cancer Cells Overexpressing CD44 with Immunoliposomes Encapsulating Glycosylated Paclitaxel. *Int. J. Mol. Sci.* **2019**, *20* (5), 1042. https://doi.org/10.3390/ijms20051042.

(40) Zheng, Z.; Ji, H.; Zong, W.; Ran, Q.; Wang, X.; Yang, X.; Zhao, Z.; Yang, C.; Xiao, Y. Construction and Characterization of Immunoliposomes Targeting Fibroblast Growth Factor Receptor 3. *AMB Express* **2019**, *9* (1), 1–9. https://doi.org/10.1186/s13568-019-0875-5.

(41) ScienceDirect Topics. Peptide - an overview https://www.sciencedirect.com/topics/medicine-and-dentistry/peptide (accessed Mar 22, 2020).

(42) Wu, H. C.; Chang, D. K. Peptide-Mediated Liposomal Drug Delivery System Targeting Tumor Blood Vessels in Anticancer Therapy. *J. Oncol.* **2010**, *2010*. https://doi.org/10.1155/2010/723798.

(43) Soudy, R.; Byeon, N.; Raghuwanshi, Y.; Ahmed, S.; Lavasanifar, A.; Kaur, K. Engineered Peptides for Applications in Cancer-Targeted Drug Delivery and Tumor Detection. *Mini-Reviews Med. Chem.* **2016**, *17* (18). https://doi.org/10.2174/1389557516666160219121836.

(44) Zhao, N.; Qin, Y.; Liu, H.; Cheng, Z. Tumor-Targeting Peptides: Ligands for Molecular Imaging and Therapy. *Anticancer. Agents Med. Chem.* **2018**, *18* (1), 74–86. https://doi.org/10.2174/1871520617666170419143459.

(45) Zafar, S.; Beg, S.; Panda, S. K.; Rahman, M.; Alharbi, K. S.; Jain, G. K.; Ahmad, F. J. Novel Therapeutic Interventions in Cancer Treatment Using Protein and Peptide-Based Targeted Smart Systems. *Seminars in Cancer Biology*. Academic Press August 20, 2019. https://doi.org/10.1016/j.semcancer.2019.08.023.

(46) Zhang, L.; Shan, X.; Meng, X.; Gu, T.; Lu, Q.; Zhang, J.; Chen, J.; Jiang, Q.; Ning, X. The First Integrins B3-Mediated Cellular and Nuclear Targeting Therapeutics for Prostate Cancer. *Biomaterials* **2019**, *223*, 119471. https://doi.org/10.1016/j.biomaterials.2019.119471.

(47) Tang, Z.; Feng, W.; Yang, Y.; Wang, Q. Gemcitabine-Loaded RGD Modified Liposome for Ovarian Cancer: Preparation, Characterization and Pharmacodynamic Studies. *Drug Des. Devel. Ther.* **2019**, *13*, 3281–3290. https://doi.org/10.2147/DDDT.S211168.

(48) Ji, T.; Lang, J.; Wang, J.; Cai, R.; Zhang, Y.; Qi, F.; Zhang, L.; Zhao, X.; Wu, W.; Hao, J.; Qin, Z.; Zhao, Y.; Nie, G. Designing Liposomes to Suppress Extracellular Matrix Expression to Enhance Drug Penetration and Pancreatic Tumor Therapy. *ACS Nano* **2017**, *11* (9), 8668–8678. https://doi.org/10.1021/acsnano.7b01026.

(49) Chen, J.; Liu, T.; Gao, J.; Gao, L.; Zhou, L.; Cai, M.; Shi, Y.; Xiong, W.; Jiang, J.; Tong, T.; Wang, H. Variation in Carbohydrates between Cancer and Normal Cell Membranes Revealed by Super-Resolution Fluorescence Imaging. *Adv. Sci.* **2016**, *3* (12), 1600270. https://doi.org/10.1002/advs.201600270.

(50) Merriam-Webster. Lectin https://www.merriam-webster.com/dictionary/lectin (accessed Mar 23, 2020).

(51) Jain, K.; Kesharwani, P.; Gupta, U.; Jain, N. K. A Review of Glycosylated Carriers for Drug Delivery. *Biomaterials*. June 2012, pp 4166–4186. https://doi.org/10.1016/j.biomaterials.2012.02.033.

(52) Xiong, M.; Lei, Q.; You, X.; Gao, T.; Song, X.; Xia, Y.; Ye, T.; Zhang, L.; Wang, N.; Yu, L. Mannosylated Liposomes Improve Therapeutic Effects of Paclitaxel in Colon Cancer Models. *J. Microencapsul.* **2017**, *34* (6), 513–521. https://doi.org/10.1080/02652048.2017.1339739.

(53) Minnelli, C.; Cianfruglia, L.; Laudadio, E.; Galeazzi, R.; Pisani, M.; Crucianelli, E.; Bizzaro, D.; Armeni, T.; Mobbili, G. Selective Induction of Apoptosis in MCF7 Cancer-Cell by Targeted Liposomes Functionalised with Mannose-6-Phosphate. *J. Drug Target.* **2018**, *26* (3), 242–251. https://doi.org/10.1080/1061186X.2017.1365873.

(54) Tian, Y.; Zhang, H.; Qin, Y.; Li, D.; Liu, Y.; Wang, H.; Gan, L. Overcoming Drug-Resistant Lung Cancer by Paclitaxel-Loaded Hyaluronic Acid-Coated Liposomes Targeted to Mitochondria. *Drug Dev. Ind. Pharm.* **2018**, *44* (12), 2071–2082. https://doi.org/10.1080/03639045.2018.1512613.

(55) Meng, S.; Su, B.; Li, W.; Ding, Y.; Tang, L.; Zhou, W.; Song, Y.; Li, H.; Zhou, C. Enhanced Antitumor Effect of Novel Dual-Targeted Paclitaxel Liposomes. *Nanotechnology* **2010**, *21* (41), 415103. https://doi.org/10.1088/0957-4484/21/41/415103.

(56) Saul, J. M.; Annapragada, A. V.; Bellamkonda, R. V. A Dual-Ligand Approach for Enhancing Targeting Selectivity of Therapeutic Nanocarriers. *J. Control. Release* **2006**, *114* (3), 277–287. https://doi.org/10.1016/j.jconrel.2006.05.028.

(57) Ke, X.; Lin, W.; Li, X.; Wang, H.; Xiao, X.; Guo, Z. Synergistic Dual-Modified Liposome Improves Targeting and Therapeutic Efficacy of Bone Metastasis from Breast Cancer. *Drug Deliv.* **2017**, *24* (1), 1680–1689. https://doi.org/10.1080/10717544.2017.1396384.

(58) Lakkadwala, S.; dos Santos Rodrigues, B.; Sun, C.; Singh, J. Biodistribution of TAT or QLPVM Coupled to Receptor Targeted Liposomes for Delivery of Anticancer Therapeutics to Brain in Vitro and in Vivo. *Nanomedicine Nanotechnology, Biol. Med.* **2020**, *23*, 102112. https://doi.org/10.1016/j.nano.2019.102112.

(59) Pu, Y.; Zhang, H.; Peng, Y.; Fu, Q.; Yue, Q.; Zhao, Y.; Guo, L.; Wu, Y. Dual-Targeting Liposomes with Active Recognition of GLUT5 and Avβ3 for Triple-Negative Breast Cancer. *Eur. J. Med. Chem.* **2019**, *183*, 111720. https://doi.org/10.1016/j.ejmech.2019.111720.

(60) Raza, A.; Rasheed, T.; Nabeel, F.; Hayat, U.; Bilal, M.; Iqbal, H. M. N. Endogenous and Exogenous Stimuli-Responsive Drug Delivery Systems for Programmed Site-Specific Release. *Molecules*. MDPI AG March 21, 2019. https://doi.org/10.3390/molecules24061117.

(61) Liberti, M. V.; Locasale, J. W. The Warburg Effect: How Does It Benefit Cancer Cells? *Trends in Biochemical Sciences*. Elsevier Ltd March 1, 2016, pp 211–218. https://doi.org/10.1016/j.tibs.2015.12.001.

(62) Boedtkjer, E.; Pedersen, S. F. The Acidic Tumor Microenvironment as a Driver of Cancer. *Annu. Rev. Physiol.* **2020**, *82* (1), 103–126. https://doi.org/10.1146/annurev-physiol-021119-034627.

(63) Chu, C. J.; Szoka, F. C. Ph-Sensitive Liposomes. *J. Liposome Res.* **1994**, *4* (1), 361–395. https://doi.org/10.3109/08982109409037050.

(64) Vila-Caballer, M.; Codolo, G.; Munari, F.; Malfanti, A.; Fassan, M.; Rugge, M.; Balasso, A.; de Bernard, M.; Salmaso, S. A PH-Sensitive Stearoyl-PEG-Poly(Methacryloyl Sulfadimethoxine)-Decorated Liposome System for Protein Delivery: An Application for Bladder Cancer Treatment. *J. Control. Release* **2016**, *238*, 31–42. https://doi.org/10.1016/j.jconrel.2016.07.024.

(65) Zhai, L. Dual PH-Responsive DOX-Encapsulated Long-Circulating Liposomes Targeting Tumor Acid Microenvironment for Treatment of Cancer. *J. Nucl. Med.* **2019**, *60* (supplement 1), 3024.

(66) Guo, X.; Cheng, Y.; Zhao, X.; Luo, Y.; Chen, J.; Yuan, W. E. Advances in Redox-Responsive Drug Delivery Systems of Tumor Microenvironment. *Journal of Nanobiotechnology*. BioMed Central Ltd. September 22, 2018, p 74. https://doi.org/10.1186/s12951-018-0398-2.

(67) Heidarli, E.; Dadashzadeh, S.; Haeri, A. State of the Art of Stimuli-Responsive Liposomes for Cancer Therapy. *Iran. J. Pharm. Res.* **2017**, *16* (4), 1273–1304. https://doi.org/10.22037/ijpr.2017.2164.

(68) Wells, C. M.; Harris, M.; Choi, L.; Murali, V. P.; Guerra, F. D.; Jennings, J. A. Stimuli-Responsive Drug Release from Smart Polymers. *Journal of Functional Biomaterials*. MDPI AG September 1, 2019. https://doi.org/10.3390/jfb10030034.

(69) Wang, Z.; Ling, L.; Du, Y.; Yao, C.; Li, X. Reduction Responsive Liposomes Based on Paclitaxel-Ss-Lysophospholipid with High Drug Loading for Intracellular Delivery. *Int. J. Pharm.* **2019**, *564*, 244–255. https://doi.org/10.1016/j.ijpharm.2019.04.060.

(70) Du, Y.; Wang, Z.; Wang, T.; He, W.; Zhou, W.; Li, M.; Yao, C.; Li, X. Improved Antitumor Activity of Novel Redox-Responsive Paclitaxel-Encapsulated Liposomes Based on Disulfide Phosphatidylcholine. *Mol. Pharm.* **2020**, *17* (1), 262–273. https://doi.org/10.1021/acs.molpharmaceut.9b00988.

(71) Fouladi, F.; Steffen, K. J.; Mallik, S. Enzyme-Responsive Liposomes for the Delivery of Anticancer Drugs. *Bioconjug. Chem.* **2017**, *28* (4), 857–868. https://doi.org/10.1021/acs.bioconjchem.6b00736.

(72) Shahriari, M.; Zahiri, M.; Abnous, K.; Taghdisi, S. M.; Ramezani, M.; Alibolandi, M. Enzyme Responsive Drug Delivery Systems in Cancer Treatment. *Journal of Controlled Release*. Elsevier B.V. August 28, 2019, pp 172–189. https://doi.org/10.1016/j.jconrel.2019.07.004.

(73) Shchegravina, E. S.; Tretiakova, D. S.; Alekseeva, A. S.; Galimzyanov, T. R.; Utkin, Y. N.; Ermakov, Y. A.; Svirshchevskaya, E. V.; Negrebetsky, V. V.; Karpechenko, N. Y.; Chernikov, V. P.; Onishchenko, N. R.; Vodovozova, E. L.; Fedorov, A. Y.; Boldyrev, I. A. Phospholipidic Colchicinoids as Promising Prodrugs Incorporated into Enzyme-Responsive Liposomes: Chemical, Biophysical, and Enzymological Aspects. *Bioconjug. Chem.* **2019**, *30* (4), 1098–1113. https://doi.org/10.1021/acs.bioconjchem.9b00051.

(74) Ji, T.; Li, S.; Zhang, Y.; Lang, J.; Ding, Y.; Zhao, X.; Zhao, R.; Li, Y.; Shi, J.; Hao, J.; Zhao, Y.; Nie, G. An MMP-2 Responsive Liposome Integrating Antifibrosis and Chemotherapeutic Drugs for Enhanced Drug Perfusion and Efficacy in Pancreatic Cancer. *ACS Appl. Mater. Interfaces* **2016**, *8* (5), 3438–3445. https://doi.org/10.1021/acsami.5b11619.

(75) Pourhassan, H.; Clergeaud, G.; Hansen, A. E.; Østrem, R. G.; Fliedner, F. P.; Melander, F.; Nielsen, O. L.; O'Sullivan, C. K.; Kjær, A.; Andresen, T. L. Revisiting the Use of SPLA2-Sensitive Liposomes in Cancer Therapy. *J. Control. Release* **2017**, *261*, 163–173. https://doi.org/10.1016/j.jconrel.2017.06.024.

(76) Liu, D.; Yang, F.; Xiong, F.; Gu, N. The Smart Drug Delivery System and Its Clinical Potential. *Theranostics*. Ivyspring International Publisher 2016, pp 1306–1323. https://doi.org/10.7150/thno.14858.

(77) Deshpande, P. P.; Biswas, S.; Torchilin, V. P. Current Trends in the Use of Liposomes for Tumor Targeting. *Nanomedicine*. Future Medicine Ltd. 2013, pp 1509–1528. https://doi.org/10.2217/nnm.13.118.

(78) Karimi, M.; Sahandi Zangabad, P.; Ghasemi, A.; Amiri, M.; Bahrami, M.; Malekzad, H.; Ghahramanzadeh Asl, H.; Mahdieh, Z.; Bozorgomid, M.; Ghasemi, A.; Rahmani Taji Boyuk, M. R.; Hamblin, M. R. Temperature-Responsive Smart Nanocarriers for Delivery of Therapeutic Agents: Applications and Recent Advances. *ACS Appl. Mater. Interfaces* **2016**, *8* (33), 21107–21133. https://doi.org/10.1021/acsami.6b00371.

(79) Motamarry, A.; Negussie, A. H.; Rossmann, C.; Small, J.; Wolfe, A. M.; Wood, B. J.; Haemmerich, D. Real-Time Fluorescence Imaging for Visualization and Drug Uptake Prediction during Drug Delivery by Thermosensitive Liposomes. *Int. J. Hyperth.* **2019**, *36* (1), 817–826. https://doi.org/10.1080/02656736.2019.1642521.

(80) Derieppe, M.; Escoffre, J.-M.; Denis de Senneville, B.; van Houtum, Q.; Rijbroek, A. B.; van der Wurff-Jacobs, K.; Dubois, L.; Bos, C.; Moonen, C. Assessment of Intratumoral Doxorubicin Penetration after Mild Hyperthermia-Mediated Release from Thermosensitive Liposomes. *Contrast Media Mol. Imaging* **2019**, 2645928. https://doi.org/10.1155/2019/2645928.

(81) Lyu, Y.; Xiao, Q.; Yin, L.; Yang, L.; He, W. Potent Delivery of an MMP Inhibitor to the Tumor Microenvironment with Thermosensitive Liposomes for the Suppression of Metastasis and Angiogenesis. *Signal Transduct. Target. Ther.* **2019**, *4* (1), 1–9. https://doi.org/10.1038/s41392-019-0054-9.

(82) Chen, M. M.; Liu, Y. Y.; Su, G. H.; Song, F. F.; Liu, Y.; Zhang, Q. Q. NIR Responsive Liposomal System for Rapid Release of Drugs in Cancer Therapy. *Int. J. Nanomedicine* **2017**, *12*, 4225–4239. https://doi.org/10.2147/IJN.S130861.

(83) Yu, Q.; Huang, T.; Liu, C.; Zhao, M.; Xie, M.; Li, G.; Liu, S.; Huang, W.; Zhao, Q. Oxygen Self-Sufficient NIR-Activatable Liposomes for Tumor Hypoxia Regulation and Photodynamic Therapy. *Chem. Sci.* **2019**, *10* (39), 9091–9098. https://doi.org/10.1039/c9sc03161h.

(84) T.S, A.; Shalumon, K. T.; Chen, J.-P. Applications of Magnetic Liposomes in Cancer Therapies. *Curr. Pharm. Des.* **2019**, *25* (13), 1490–1504. https://doi.org/10.2174/1389203720666190521114936.

(85) De Cuyper, M.; Joniau, M. Magnetoliposomes - Formation and Structural Characterization. *Eur. Biophys. J.* **1988**, *15* (5), 311–319. https://doi.org/10.1007/BF00256482.

(86) Hardiansyah, A.; Destyorini, F.; Irmawati, Y.; Yang, M. C.; Liu, C. M.; Chaldun, E. R.; Yung, M. C.; Liu, T. Y. Characterizations of Doxorubicin-Loaded PEGylated Magnetic Liposomes for Cancer Cells Therapy. *J. Polym. Res.* **2019**, *26* (12), 1–8. https://doi.org/10.1007/s10965-019-1964-5.

(87) Lu, Y. J.; Chuang, E. Y.; Cheng, Y. H.; Anilkumar, T. S.; Chen, H. A.; Chen, J. P. Thermosensitive Magnetic Liposomes for Alternating Magnetic Field-Inducible Drug Delivery in Dual Targeted Brain Tumor Chemotherapy. *Chem. Eng. J.* **2019**, *373*, 720–733. https://doi.org/10.1016/j.cej.2019.05.055.

(88) Schroeder, A.; Kost, J.; Barenholz, Y. Ultrasound, Liposomes, and Drug Delivery: Principles for Using Ultrasound to Control the Release of Drugs from Liposomes. *Chem. Phys. Lipids* **2009**, *162* (1–2), 1–16. https://doi.org/10.1016/j.chemphyslip.2009.08.003.

(89) Frenkel, V. Ultrasound Mediated Delivery of Drugs and Genes to Solid Tumors. *Adv. Drug Deliv. Rev.* **2008**, *60* (10), 1193–1208. https://doi.org/10.1016/j.addr.2008.03.007.

(90) Richardson, E. S.; Pitt, W. G.; Woodbury, D. J. The Role of Cavitation in Liposome Formation. *Biophys. J.* **2007**, *93* (12), 4100–4107. https://doi.org/10.1529/biophysj.107.104042.

(91) Delalande, A.; Kotopoulis, S.; Postema, M.; Midoux, P.; Pichon, C. Sonoporation: Mechanistic Insights and Ongoing Challenges for Gene Transfer. *Gene* **2013**, *525* (2), 191–199. https://doi.org/10.1016/j.gene.2013.03.095.

(92) Pitt, W. G.; Husseini, G. A.; Staples, B. J. Ultrasonic Drug Delivery – a General Review. *Expert Opin. Drug Deliv.* **2004**, *1* (1), 37–56. https://doi.org/10.1517/17425247.1.1.37.

(93) Mullick Chowdhury, S.; Lee, T.; Willmann, J. K. Ultrasound-Guided Drug Delivery in Cancer. *Ultrasonography* **2017**, *36* (3), 171–184. https://doi.org/10.14366/usg.17021.

(94) Karimi, M.; Ghasemi, A.; Zangabad, P. S.; Rahighi, R.; Masoud, S.; Basri, M.; Mirshekari, H.; Amiri, M.; Pishabad, Z. S.; Aslani, A.; Ghosh, D.; Beyzavi, A.; Vaseghi, A.; Aref, A. R.; Haghani, L.; Bahrami, S.; Hamblin, M. R.; Village, O.; Cancer, D.; Hospital, M. G. Smart Micro/Nanoparticles in Stimulus-Responsive Drug/Gene Delivery Systems. *HHS Public Access* **2017**, *45* (5), 1457–1501. https://doi.org/10.1039/c5cs00798d.Smart.

(95) Xin, Y.; Qi, Q.; Mao, Z.; Zhan, X. PLGA Nanoparticles Introduction into Mitoxantrone-Loaded Ultrasound-Responsive Liposomes: In Vitro and in Vivo Investigations. *Int. J. Pharm.* **2017**, *528* (1–2), 47–54. https://doi.org/10.1016/j.ijpharm.2017.05.059.

(96) Santos, M. A.; Goertz, D. E.; Hynynen, K. Focused Ultrasound Hyperthermia Mediated Drug Delivery Using Thermosensitive Liposomes and Visualized with in Vivo Two-Photon Microscopy. *Theranostics* **2017**, *7* (10), 2718–2731. https://doi.org/10.7150/thno.19662.

(97) Xing, S.; Zhang, X.; Luo, L.; Cao, W.; Li, L.; He, Y.; An, J.; Gao, D. Doxorubicin/Gold Nanoparticles Coated with Liposomes for Chemo-Photothermal Synergetic Antitumor Therapy. *Nanotechnology* **2018**, *29* (40), 405101. https://doi.org/10.1088/1361-6528/AAD358.

(98) Chen, M. M.; Song, F. F.; Feng, M.; Liu, Y.; Liu, Y. Y.; Tian, J.; Lv, F.; Zhang, Q. Q. PH-Sensitive Charge-Conversional and NIR Responsive Bubble-Generating Liposomal System for Synergetic Thermo-Chemotherapy. *Colloids Surfaces B Biointerfaces* **2018**, *167*, 104–114. https://doi.org/10.1016/j.colsurfb.2018.04.001.

(99) Wang, M.; Liu, Y.; Zhang, X.; Luo, L.; Li, L.; Xing, S.; He, Y.; Cao, W.; Zhu, R.; Gao, D. Gold Nanoshell Coated Thermo-PH Dual Responsive Liposomes for Resveratrol Delivery and Chemo-Photothermal Synergistic Cancer Therapy. *J. Mater. Chem. B* **2017**, *5* (11), 2161–2171. https://doi.org/10.1039/c7tb00258k.

(100) Shirmardi Shaghasemi, B.; Virk, M. M.; Reimhult, E. Optimization of Magneto-Thermally Controlled Release Kinetics by Tuning of Magnetoliposome Composition and Structure. *Sci. Rep.* **2017**, *7* (1), 1–10. https://doi.org/10.1038/s41598-017-06980-9.

(101) Lee, J. M.; Park, H.; Oh, K. T.; Lee, E. S. PH-Responsive Hyaluronated Liposomes for Docetaxel Delivery. *Int. J. Pharm.* **2018**, *547* (1–2), 377–384. https://doi.org/10.1016/j.ijpharm.2018.06.028.

(102) Yang, Y.; Yang, Y.; Xie, X.; Xu, X.; Xia, X.; Wang, H.; Li, L.; Dong, W.; Ma, P.; Liu, Y. Dual Stimulus of Hyperthermia and Intracellular Redox Environment Triggered Release of SiRNA for Tumor-Specific Therapy. *Int. J. Pharm.* **2016**, *506* (1–2), 158–173. https://doi.org/10.1016/j.ijpharm.2016.04.035.

(103) Patra, J. K.; Das, G.; Fraceto, L. F.; Campos, E. V. R.; Rodriguez-Torres, M. D. P.; Acosta-Torres, L. S.; Diaz-Torres, L. A.; Grillo, R.; Swamy, M. K.; Sharma, S.; Habtemariam, S.; Shin, H. S. Nano Based Drug Delivery Systems: Recent Developments and Future Prospects. *J. Nanobiotechnology* **2018**, *16* (71). https://doi.org/10.1186/s12951-018-0392-8.

(104) Ekdawi, S. N.; Jaffray, D. A.; Allen, C. Nanomedicine and Tumor Heterogeneity: Concept and Complex Reality. *Nano Today*. Elsevier B.V. August 1, 2016, pp 402–414. https://doi.org/10.1016/j.nantod.2016.06.006.

(105) Moghimi, S. M.; Farhangrazi, Z. S. Just so Stories: The Random Acts of Anti-Cancer Nanomedicine Performance. *Nanomedicine Nanotechnology, Biol. Med.* **2014**, *10* (8), 1661–1666. https://doi.org/10.1016/j.nano.2014.04.011.

(106) Denison, T. A.; Bae, Y. H. Tumor Heterogeneity and Its Implication for Drug Delivery. *J. Control. Release* **2012**, *164* (2), 187–191. https://doi.org/10.1016/j.jconrel.2012.04.014.

(107) Dagogo-Jack, I.; Shaw, A. T. Tumour Heterogeneity and Resistance to Cancer Therapies. *Nature Reviews Clinical Oncology*. Nature Publishing Group February 1, 2018, pp 81–94. https://doi.org/10.1038/nrclinonc.2017.166.

(108) Kydd, J.; Jadia, R.; Velpurisiva, P.; Gad, A.; Paliwal, S.; Rai, P. Targeting Strategies for the Combination Treatment of Cancer Using Drug Delivery Systems. *Pharmaceutics*. MDPI AG December 1, 2017. https://doi.org/10.3390/pharmaceutics9040046.

(109) Nakamura, H.; Jun, F.; Maeda, H. Development of Next-Generation Macromolecular Drugs Based on the EPR Effect: Challenges and Pitfalls. *Expert Opinion on Drug Delivery*. Informa Healthcare January 1, 2015, pp 53–64. https://doi.org/10.1517/17425247.2014.955011.

(110) Pauli, G.; Tang, W. L.; Li, S. D. Development and Characterization of the Solvent-Assisted Active Loading Technology (SALT) for Liposomal Loading of Poorly Water-Soluble Compounds. *Pharmaceutics*. MDPI AG September 1, 2019. https://doi.org/10.3390/pharmaceutics11090465.

(111) Na, K.; Liu, K.; Yu, J.; Wang, X.; Li, M.; Tian, C.; He, H.; He, Y.; Wang, Y. A Solvent-Assisted Active Loading Technology to Prepare Gambogic Acid and All-Trans Retinoic Acid Co-Encapsulated Liposomes for Synergistic Anticancer Therapy. *Drug Deliv. Transl. Res.* **2020**, *10* (1), 146–158. https://doi.org/10.1007/s13346-019-00669-4.

(112) Malone, E. R.; Oliva, M.; Sabatini, P. J. B.; Stockley, T. L.; Siu, L. L. Molecular Profiling for Precision Cancer Therapies. *Genome medicine*. NLM (Medline) January 14, 2020, p 8. https://doi.org/10.1186/s13073-019-0703-1.

(113) Le Tourneau, C.; Borcoman, E.; Kamal, M. Molecular Profiling in Precision Medicine Oncology. *Nat. Med.* **2019**, *25* (5), 711–712. https://doi.org/10.1038/s41591-019-0442-2.

(114) Sicklick, J. K.; Kato, S.; Okamura, R.; Schwaederle, M.; Hahn, M. E.; Williams, C. B.; De, P.; Krie, A.; Piccioni, D. E.; Miller, V. A.; Ross, J. S.; Benson, A.; Webster, J.; Stephens, P. J.; Lee, J. J.; Fanta, P. T.; Lippman, S. M.; Leyland-Jones, B.; Kurzrock, R. Molecular Profiling of Cancer Patients Enables Personalized Combination Therapy: The I-PREDICT Study. *Nature Medicine*. Nature Publishing Group May 1, 2019, pp 744–750. https://doi.org/10.1038/s41591-019-0407-5.

(115) Rothwell, D. G.; Ayub, M.; Cook, N.; Thistlethwaite, F.; Carter, L.; Dean, E.; Smith, N.; Villa, S.; Dransfield, J.; Clipson, A.; White, D.; Nessa, K.; Ferdous, S.; Howell, M.; Gupta, A.; Kilerci, B.; Mohan, S.; Frese, K.; Gulati, S.; Miller, C.; Jordan, A.; Eaton, H.; Hickson, N.; O'Brien, C.; Graham, D.; Kelly, C.; Aruketty, S.; Metcalf, R.; Chiramel, J.; Tinsley, N.; Vickers, A. J.; Kurup, R.; Frost, H.; Stevenson, J.; Southam, S.; Landers, D.; Wallace, A.; Marais, R.; Hughes, A. M.; Brady, G.; Dive, C.; Krebs, M. G. Utility of CtDNA to Support Patient Selection for Early Phase Clinical Trials: The TARGET Study. *Nature Medicine*. Nature Publishing Group May 1, 2019, pp 738–743. https://doi.org/10.1038/s41591-019-0380-z.

(116) Appierto, V.; Di Cosimo, S.; Reduzzi, C.; Pala, V.; Cappelletti, V.; Daidone, M. G. How to Study and Overcome Tumor Heterogeneity with Circulating Biomarkers: The Breast Cancer Case. *Seminars in Cancer Biology*. Academic Press June 1, 2017, pp 106–116. https://doi.org/10.1016/j.semcancer.2017.04.007.

(117) Bartelink, I. H.; Jones, E. F.; Shahidi-Latham, S. K.; Lee, P. R. E.; Zheng, Y.; Vicini, P.; van 't Veer, L.; Wolf, D.; Iagaru, A.; Kroetz, D. L.; Prideaux, B.; Cilliers, C.; Thurber, G. M.; Wimana, Z.; Gebhart, G. Tumor Drug Penetration Measurements Could Be the Neglected Piece of the Personalized Cancer Treatment Puzzle. *Clinical Pharmacology and Therapeutics*. Nature

Publishing Group July 1, 2019, pp 148–163. https://doi.org/10.1002/cpt.1211.

(118) Bullock, J. M.; Lin, T.; Bilic, S. Clinical Pharmacology Tools and Evaluations to Facilitate Comprehensive Dose Finding in Oncology: A Continuous Risk-Benefit Approach. *J. Clin. Pharmacol.* **2017**, *57*, S105–S115. https://doi.org/10.1002/jcph.908.

(119) Shord, S. S. The Role of Clinical Pharmacology in Oncology Dose Selection: Advances and Opportunities in Personalized Medicine. *J. Clin. Pharmacol.* **2017**, *57*, S99–S104. https://doi.org/10.1002/jcph.922.

(120) Zhao, B.; Schwatrz, L. H. Imaging in Clinical Trials. In *Oncology clinical trials: successful design, conduct, and analysis*; Kelly, W. K., Halabi, S., Eds.; Springer Publishing Company, 2018; pp 239–249.

(121) Gerwing, M.; Herrmann, K.; Helfen, A.; Schliemann, C.; Berdel, W. E.; Eisenblätter, M.; Wildgruber, M. The Beginning of the End for Conventional RECIST — Novel Therapies Require Novel Imaging Approaches. *Nature Reviews Clinical Oncology*. Nature Publishing Group July 1, 2019, pp 442–458. https://doi.org/10.1038/s41571-019-0169-5.

(122) Majidinia, M.; Mirza-Aghazadeh-Attari, M.; Rahimi, M.; Mihanfar, A.; Karimian, A.; Safa, A.; Yousefi, B. Overcoming Multidrug Resistance in Cancer: Recent Progress in Nanotechnology and New Horizons. *IUBMB Life* **2020**, *72* (5), 855–871. https://doi.org/10.1002/iub.2215.

(123) Afadzi, M.; Davies, C. de L.; Hansen, Y. H.; Johansen, T.; Standal, Ø. K.; Hansen, R.; Måsøy, S. E.; Nilssen, E. A.; Angelsen, B. Effect of Ultrasound Parameters on the Release of Liposomal Calcein. *Ultrasound Med. Biol.* **2012**, *38* (3), 476–486. https://doi.org/10.1016/j.ultrasmedbio.2011.11.017.

(124) Husseini, G. A.; Myrup, G. D.; Pitt, W. G.; Christensen, D. A.; Rapoport, N. Y. Factors Affecting Acoustically Triggered Release of Drugs from Polymeric Micelles. *J. Control. Release* **2000**, *69* (1), 43–52. https://doi.org/10.1016/s0168-3659(00)00278-9.

(125) Pitt, W. G.; Husseini, G. A.; Roeder, B. L.; Dickinson, D. J.; Warden, D. R.; Hartley, J. M.; Jones, P. W. Preliminary Results of Combining Low Frequency Low Intensity Ultrasound and Liposomal Drug Delivery to Treat Tumors in Rats. *J. Nanosci. Nanotechnol.* **2011**, *11* (3), 1866–1870. https://doi.org/10.1166/jnn.2011.3117.

(126) Schroeder, A.; Avnir, Y.; Weisman, S.; Najajreh, Y.; Gabizon, A.; Talmon, Y.; Kost, J.; Barenholz, Y. Controlling Liposomal Drug Release with Low Frequency Ultrasound: Mechanism and Feasibility. *Langmuir* **2007**, *23* (7), 4019–4025. https://doi.org/10.1021/LA0631668.

(127) Pong, M.; Umchid, S.; Guarino, A. J.; Lewin, P. A.; Litniewski, J.; Nowicki, A.; Wrenn, S. P. In Vitro Ultrasound-Mediated Leakage from Phospholipid Vesicles. *Ultrasonics* **2006**, *45* (1–4), 133–145. https://doi.org/10.1016/j.ultras.2006.07.021.

(128) Marin, A.; Muniruzzaman, M.; Rapoport, N. Acoustic Activation of Drug Delivery from Polymeric Micelles: Effect of Pulsed Ultrasound. *J. Control. Release* **2001**, *71* (3), 239–249. https://doi.org/10.1016/s0168-3659(01)00216-4.

(129) Wirth, T.; Ylä-Herttuala, S. Gene Therapy Used in Cancer Treatment. *Biomedicines*. MDPI AG June 1, 2014, pp 149–162. https://doi.org/10.3390/biomedicines2020149.

(130) Amer, M. H. Gene Therapy for Cancer: Present Status and Future Perspective. *Mol. Cell. Ther.* **2014**, *2* (1), 27. https://doi.org/10.1186/2052-8426-2-27.

(131) Kamta, J.; Chaar, M.; Ande, A.; Altomare, D. A.; Ait-Oudhia, S. Advancing Cancer Therapy with

Present and Emerging Immuno-Oncology Approaches. *Front. Oncol.* **2017**, *7* (APR). https://doi.org/10.3389/fonc.2017.00064.

(132) Roma-rodrigues, C.; Rivas-garcía, L.; Baptista, P. V.; Fernandes, A. R. Gene Therapy in Cancer Treatment: Why Go Nano? *Pharmaceutics*. MDPI AG March 1, 2020. https://doi.org/10.3390/pharmaceutics12030233.

(133) Chen, J.; Guo, Z.; Tian, H.; Chen, X. Production and Clinical Development of Nanoparticles for Gene Delivery. *Molecular Therapy - Methods and Clinical Development*. Elsevier Inc March 16, 2016, p 16023. https://doi.org/10.1038/mtm.2016.23.

(134) Sun, W.; Shi, Q.; Zhang, H.; Yang, K.; Ke, Y.; Wang, Y.; Qiao, L. Advances in the Techniques and Methodologies of Cancer Gene Therapy. *Discov. Med.* **2019**, *27* (146), 45–55.

Table 1: Summary of recent studies focusing on dual-targeted liposomes.

Moiety	Payload	Cancer cell line	Animal model	Main findings	Ref.
Asp_8 and Folate	DOX	Breast cancer (MDA-MB-231) cells	-	1. The optimal density of Asp_8 and Folate on the liposomes was chosen to be 15% and 10% (molar ratio), respectively. 2. DOX-A/F-LS treatment prolonged median survival time by 1.7, 1.4, 1.2, and 1.3-times compared to the treatment groups of physiological saline, free DOX, DOX-A-LS, and DOX-F-LS, respectively.	(*57*)
Tf and Pen	DOX and Erlotinib	Glioblastoma (U87) cells	Male/Female nude mice	1. Tf-Pen liposomes demonstrated ~12 and 3.3-fold increase in DOX and erlotinib accumulation in mice brains. 2. Tf-Pen liposomes achieved around 90% tumor regression with an increase in the median survival time (36 days) and no toxicity.	(*135*)
Tf, TAT and QLPVM	DOX and Erlotinib	Glioblastoma (U87), brain endothelial (bEnd.3) and glial cells	Male/female nude mice	1. The biodistribution profile of Tf-CPP liposomes showed more than 10- and 2.7-fold increase in DOX and erlotinib accumulation in mice brain.	(*58*)
Fru and RGD	PXT	Breast cancer (MDA-MB-231 and 4T1) cells	Balb/C mice	1. The cellular uptake of Fru-RGD-Lip by MDA-MB-231 and 4T1 cells was 3.19- and 3.23-fold more than that of uncoated liposomes. 2. The uptake of Fru+RGD-Lip was slightly lower, giving a 2.81- and 2.90-fold increase than that of Lip in two cell lines, respectively.	(*59*)

Moiety	Payload	Cancer cell line	Animal model	Main findings	Ref.
Tf and R8	DOX	Ovarian carcinoma (A2780) cells	Immunodeficient female Ncr NU/NU nude mice	1. Dual DOX-L showed approximately 30% and 10% more cell death than R8 DOX-L. 2. At the end of the study, the tumor volumes were 900.3 ± 60.0 mm^3 for control tumors, 848.6 ± 218.2 mm^3 for Free DOX, 268.4 ± 19.2 mm^3 for PL DOX-L, 224.8 ± 50.3 mm^3 for Tf DOX-L, 281.6 ± 51.6 mm^3 for R8 DOX-L and 124.9 ± 33.69 mm^3 for Dual DOX-L.	(*136*)
T7 and ^{D}A7R	DOX and VCR	Human umbilical vein endothelial cells (HUVECs), glioma C6 cells, and mouse brain endothelial bEnd.3	Female ICR mice	1. The co-delivery of drugs (DOX+VCR) by the T7/ ^{D}A7R-LS increased the cytotoxicity, with an IC_{50} of 3.54μg/mL, compared to 4.12, 4.09, and 4.6 μg/mL for T7-LS, ^{D}A7R-LS, and N-L. 2. The % survival of C6 cells after addition of free DOX+free VCR, N-LS, ^{D}A7R-LS, T7-LS, and T7/^{D} A7R-LS, was 97.88 ± 2.53, 92.86 ± 3.33, 91.14 ± 1.74, 39.64 ± 2.94, and 40.05 ± 2.12%, respectively.	(*137*)
Angiopep-2 and A15 aptamers	Survivin siRNA and PTX	Human glioblastoma astrocytoma (U251) cells	Male BALB/c nude mice	1. DP-CLPs–PTX–siRNA nanocomplex induced selective apoptosis of $CD133^{+}$ glioma stem cells. 2. The liposomes markedly inhibited tumorigenesis, and improved survival rates.	(*138*)
Glu and Vc	PTX	Glioma (C6) cells	Kunming mice	1. The cellular uptake of CFPE-labeled Glu-Vc-Lip on $GLUT_1$- and $SVCT_2$-overexpressed C6 cells was 4.79-, 1.95-, 4.00- and 1.53-fold higher than that of Lip, Glu-Lip, Vc-Lip and Glu + Vc-Lip. 2. The *in vivo* uptake efficiency was enhanced by 7.53-fold to that of free PTX.	(*139*)

Moiety	Payload	Cancer cell line	Animal model	Main findings	Ref.
Glu_6 and RGD	PTX	Breast cancer (MDA-MB-231) cells	Female Balb/c nu mice	1. The *in vivo* targeting showed that PTX-Glu6-RGD-Lip favored accumulation in the metastatic bones.	(*140*)
Glu_6 and FA	PTX	Breast cancer (MDA-MB-231 and MCF10A) cells	Female Balb/c nu mice	1. The (AUC_{0-t}) increased by about 1.66-time for PTX-Glu6-FA-Lip compared to free PTX. 2. Following the injection of PTX-Glu6-FA-Lip, PTX was nearly 10 times higher than with PTX injected, 2–6 times higher than with PTX-Lip injected, and 1–3 times higher than with PTX-Glu6-Lip, PTX-FA-Lip and PTX-Glu6+FA-Lip.	(*141*)
HA and FA	siBcl-2	Cervical carcinoma (HeLa) cells	Femal nude mice	1. Fluorescence intensity of HA/FA-Lip/$siRNA^{FAM}$ was 2.1 times higher than Lip/$siRNA^{FAM}$ group and 1.8 times that of HA-Lip/$siRNA^{FAM}$. 2. HA-FA-Lip/siBcl-2 group showed good silencing effect and low cytotoxicity when the siRNA concentration was set to 100 nM.	(*142*)

Abbreviations: **Asp_8,** Aspartate**; DOX,** Doxorubicin**; Tf,** Transferrin**; Pen,** Penetratin**; Fru,** Fructose**; PXT,** Paclitaxel**; R8,** Octaarginine**; VCR,** Vincristine**; Glu,** Glucose**; Vc,** Vitamin C**; Glu_6,** Glutamic oligopeptide; **HA**, Hyaluronic acid; **FA**, Folic acid.

Table 2: Summary of recent studies focusing on dual/multi-stimuli responsive liposomes.

Stimuli	Payload	Cancer cell line	Animal model	Main findings	Ref.
Temperature and Magnetic	Fe_3O_4 MNPs and DOX	Cervical carcinoma (HeLa) cells	n/a	1. DOX released from the MagABC liposomes at 37°C was about 20%; however, at 42°C, it increased to approximately 45%. 1. The relative fluorescence intensity of Hela cells was 7.5% and 64.2% after incubation with the MagABC liposomes at 37 and 42 °C, respectively, compared to 11.1% and 19.9% for ABC liposomes alone.	(*143*)
NIR Light and Temperature	DOX and Au NPs	Cervical carcinoma (HeLa) cells	Female Kunming mice	2. The tumor inhibition rate of Au/DOX-Lips NIR reached 85.81%, which was higher than that of Au/DOX-Lips (56.85%) and free DOX (35.37%).	(*97*)
pH and NIR light	Cypate, DOX and NH_4HCO_3	Mammary carcinoma (4T1) cells	Female BALA/c nude mice	1. At pH 5.0, the DOX release (after NIR exposure) from PSD/DOX/Cypate-BTSL and PSD/DOX/Cypate-L were 87.8% and 52.7% respectively.	(*98*)
NIR light, Temperature and pH	Res	Cervical carcinoma (HeLa) cells	n/a	1. About 57.6 % of Res was released at a pH of 5.0 compared with only 20.5 % at pH 7.4. 2. Without NIR, the release from GNS-CTS-Res-lips was only 5.7 % (pH 7.4) and 13.7 % (pH 5.0). 3. The therapeutic value of Res and NIR was 57.3 %, which is higher than Res alone (29.6 %) or sole photothermal therapy (42.6 %), but lower than the measured the therapeutic efficacy of the Res-NIR-Temp-pH treatment group (81.1 %), proving the distinct, synergistic effect of chemophotothermal therapy in *vitro*.	(*99*)

Stimuli	Payload	Cancer cell line	Animal model	Main findings	Ref.
Temperature and Magnetic	SPION and calcein	n/a	n/a	1. For 4wt% SPIONs, ~ 90% of calcein was released while when 2 wt% SPION were incorporated, only 28% was released.	(*100*)
NIR light and Temperature	Cisplatin and ICG	Breast cancer (MDA-MB-231) cells	n/a	1. The liposomes showed improved inhibitory effect (3.05% cell viability) with added NIR, compared to free cisplatin (28.41%) or treatment without NIR (11.24%).	(*144*)
Magnetic and enzyme	ICG	Oral squamous cell carcinoma (SCC9) cells and Hypopharyngeal squamous cell carcinoma (UD SCC2) cells	NMRI-Foxn1nu/foxn1nu female Mice	1. AMF with SMase increased the FMT fluorescence compared with only SMase. 2. UDSCC2 cells are significantly more sensitive than SCC9 in trigging ASMase activity under high doses of irradiation. 3. Significant increases of SMase activity and decrease of cell viability were observed with treatment time at higher dose cisplatin.	(*145*)
NIR light, pH and Temperature	OA	Human osteosarcoma (143B) cells	-	1. At pH 7.4, the release rates of GNOLs reached 42 ± 1%, but at pH 5.5 they release 53± 1%. 2. The drug release rate of the NIR group reached 92 ± 1%, while the non-NIR group was only 69 ± 1%. 3. The 143B cells treated with GNOLs exhibited tumor inhibition rates of 73.74 ± 1.32%. 4. The inhibition rates of GNOLs were 73.74 ± 1.32% without NIR, and 86.91 ± 2.53% with NIR. 5. In *in vivo* experiments with GNOLs and NIR showed the highest antitumor effect with an inhibition rate of 79.65%.	(*146*)

Stimuli	Payload	Cancer cell line	Animal model	Main findings	Ref.
NIR light and Temperature	Sunitinib and IR780 dye	Mammary carcinoma (4T1) cells and Human Umbilical Vein Endothelial (HUVEC) Cells	Syngeneic female BALB/c	1. Less than 30% was released from Lip-IR780-Sunitinib in medium with a pH of 5.0, 6.8 or 7.4 indicating the stability of liposomes under different pH conditions. 2. The release with NIR was about 3-fold higher than that without laser (from 11.6% to 33.6%). 3. The cell viability of Lip-IR780 NIR and Lip-IR780-Sunitinib with NIR dropped to about 50%. 4. Sunitinib/laser was the most effective at suppressing tumor angiogenesis among all the treatment groups (MVD of 80.7%).	(*147*)
pH and Temperature	DiIC18(5) and Calcein	Human hepatoma (HepG2) cells	n/a	1. The release of liposomes from the hydrogel was temperature and enzymatic responsive.	(*148*)
pH and Temperature	DOX	Human aortic adventitial fibroblasts (AoAF) and Murine NIH3T3 cells	n/a	1. Enzymatic degradation began several hrs after exposure to MMP-1, while DOX release occured almost immediately following hyperthermic stimulus, with complete release after 48 hrs.	(*149*)

Abbreviations: **Au NPs**, Gold nanoparticles; **NIR**, Near-infrared; **Res**, Resveratrol; **n/a**; Not applicable; **SPION**, Superparamagnetic iron oxide nanoparticles; **ICG**, Indocyanine green; **AMF**, Alternating magnetic field; **MNP**, Magnetic nanoparticle; **MagABC**, Magnetic ammonium bicarbonate; **CPT-11**, Camptosar; **TML**, Thermosensitive magnetic liposome; **OA**, Oleanolic acid; **GNOL**, Gold nanoshells coated oleanolic acid loaded liposome; **MVD**, Microvessel density; **DiIC18(5)**, 1,1-dioctadecyl-3,3,3,3-tetramethylindodicarbocyanine perchlorate.

Table 3: Summary of recent studies focusing on stimuli-triggered targeted liposomes.

Stimuli	Moiety	Payload	Cancer cell line	Animal model	Main findings	Ref.
Magnetic and Temperature	CET	CPT-11 and citric acid-coated Fe_3O_4 MNPs	Human primary glioblastoma (U87) cells	Balb/c nude mice	1. Around 19% CPT-11 was released *in vitro* without AMF, contrastingly around 97% drug released with AMF (at 43°C). 2. The cell viability of the TML-CPT-11 group was reduced from ~ 80% (37 °C) to ~40% (43 °C). 3. The median survival time of control and TMLCET was 20 and 21 days, respectively. For CPT-11 loaded liposomes, TML-CPT-11 and TML-CPT-11- CET groups showed median survival times of 27 and 28 days, respectively. The median survival increased to 30 days with magnetic guidance, which further increased to 33.5 days when augmented with AMF treatment.	(*87*)
pH	HA-g-DEAP	DTX	Human colon carcinoma (HCT-116) cells	n/a	1. Compared to HA-g-$DEAP_{0.15}$ and HA-g-$DEAP_{0.25}$, HA-g-$DEAP_{0.40}$ was the best pH responsive formulation. 2. HA-g-$DEAP_{0.40}$-lip displayed a higher cumulative DTX release at pH 6.5 than that at pH 7.4. 3. TX-loaded HA-g-$DEAP_{0.40}$-lip significantly reduced cell viability in HCT-116 cells. 4. HA-g-$DEAP_{0.40}$-lip showed the highest hemolysis effect at pH 6.5.	(*101*)
pH	ErbB2 antibody Fab	DOX	Breast cancer (HCC1954) and (MDA-MB-468) cells	Female BALB/c nu/nu mice	1. The cell association of Fab′-GGLG liposomes increased 10-fold in comparison to GGLG liposomes. 2. A significantly enhanced tumor growth inhibition was obtained in an ErbB2-overexpressing breast cancer-bearing mouse model.	(*150*)
US	iRGD	DOX	Mammary carcinoma cells (4T1), human breast adenocarcinoma (MCF-7) cell and Human Umbilical Vein Endothelial (HUVEC) Cells	n/a	1. DOX from iRGD-LTSL-DOX rapidly penetrated tumor interstitial space after HIFU-triggered heat treatment.	(*151*)

Stimuli	Moiety	Payload	Cancer cell line	Animal model	Main findings	Ref.
US	^{111}In-EGF	DOX	Human breast Cancer (MDA-MB-468 and MCF7) cells	Female athymic nude mice	1. Cell killing was higher in MDA-MB-468 than MCF7 cells. 2. Increased tumor uptake by 66% in the MDA-MB-468 cell line.	(*152*)
US	HSA	Calcein	Breast cancer cell lines (MDA-MB-231 and MCF-7)	n/a	1. Calcein uptake by the cancer cells was enhanced following sonication.	(*153*)
US	ES	Calcein	Breast cancer (MDA-MB-231 and MCF-7) cells	n/a	1. The exposure to LFUS revealed an enhanced calcein uptake by the cells.	(*154*)
pH	$H_7K(R_2)_2$ peptide	DOX	Rat glioma (C6) cells and human glioblastoma (U87-MG) cells	Orthotopic tumor-bearing nude mice	1. For DOX-PSL-$H_7K(R_2)_2$ and DOX-PSL groups, the release of DOX in pH 5.5, 6.0 and 6.5 buffer solutions was faster than that in pH 7.4. 2. The cellular level for coumarin-6-PSL-$H_7K(R_2)_2$ and coumarin-6-PSL was about 1.7- and 1.2-fold higher than that for coumarin-6-SSL at pH 6.8. However, at pH 7.4, the fluorescence of coumarin-6-PSL-$H_7K(R_2)_2$, coumarin-6-PSL and coumarin-6-SSL was almost identical. 3. The median survival time of mice treated with DOX-PSL-$H_7K(R_2)_2$ (39 days) was longer than that of mice treated with DOX-SSL (31 days) and DOX-PSL (35 days).	(*155*)
Redox	HA	DOX	Osteosarcoma (MG63) and liver (LO2) cells	BALB/c nude	1. In the medium without GSH, only 30% was released from the HA-lip, adding 20μM GHS increased the release to 32.8%; however, adding 10mM GHS triggered a burst release of DOX with >60%. 2. The liposomes had more pronounced cytotoxicity to MG63 cells than to normal liver cells. 3. Chol-SS-mPEG/HA-L resulted in most significant inhibition of tumor growth compared with all other liposomes or free DOX.	(*156*)

Stimuli	Moiety	Payload	Cancer cell line	Animal model	Main findings	Ref.
pH	Polyarginine	siRNA	Breast cancer (MCF-7) and human lung carcinoma (A549) cells	n/a	1. When pretreated under acidic conditions (pH 6.2), siRNA-loaded liposomes showed elevated level of cellular uptake and apoptosis compared to those incubated at pH 7.4. 2. The results of cell uptake, apoptosis, and gene expression analyses under acidic conditions for the ACPP-L group were not comparable to those of the CPP-L group.	(*157*)
pH and Magnetic	$H_7K(R_2)_2$	PTX	Human breast carcinoma (MDA-MB-231) cells	Female BALB/c nude mice	1. The released PTX from PTX/SPIO-SSL-$H_7K(R_2)_2$ in both buffer solutions of pH 6.8 and 7.4 was almost identical. 2. The IC_{50} value of the PTXSSL-$H_7K(R_2)_2$ group at pH 6.8 (7.24±0.57 μM), was significantly reduced, compared with that at pH 7.4 (31.97±4.94 μM). 3. The tumor growth inhibition in the PTX-SSL-, PTX/SPIO-SSL-, and PTX/SPIO-SSL-$H_7K(R_2)_2$ groups was about 70%, 70%, and 90%, respectively.	(*158*)
pH	RGD and [D]-H_6L_9	PTX	Colon carcinoma (C26) and breast cancer (MCF-7) cells	Balb/C mice	1. Under pH 6.3, (R+D)-Lip could be taken up by C26 cells with improved efficiency. 2. (R+ D)-Lip resulted in significant tumor growth suppression. 3. The body weights of all groups hardly dropped during the treatment, implying that all the PTX-loaded liposomes showed little in vivo toxicity.	(*159*)
pH and Enzyme	Anti-PD-L1 peptide and MMPs responsive moiety	DOX	mouse melanoma model (B16F10) cells	Female C57BL/6 mice	1. LPDp achieved the optimal tumor suppression efficiency (~78.7%), which demonstrated the significantly enhanced antitumor effect than that of LPp (~57.5%) as well as that of LD (<40%).	(*160*)
pH	CD25 antibody	IL-2, PD-L1, and IQ	Lung metastasis tumor (B16BL/6) model cells	C57BL6 mice	1. CD25-Lipo (IL/PL/IQ)+Treg cells suppressive effect on effector $CD4^+$ T cell proliferation was 77.0% which was similar to the control group (79.4%) without Treg cells. However, iso-Lipo (IL/PL/IQ) + Treg cells and Treg cells alone, reduced the percentage of proliferation to 47.5 and 49.4%, respectively. 2. Lower tumor weight was identified in mice treated with CD25- Lipo (IL/PL/IQ) Treg compared to those treated with isoLipo (IL/PL/IQ) plus Treg.	(*161*)

Stimuli	Moiety	Payload	Cancer cell line	Animal model	Main findings	Ref.
Redox and pH	CS and HA	IAP inhibitor survivin-shRNA gene and HAase	Human breast cancer (MDA-MB-231 & MCF-7) cells and mouse embryonic fibroblast (NIH/3T3) cells	BALB/c nude mice	1. The uptake of HCLR incubated in pH 6.5 was ~85%, which was greater than that in pH 7.4. 2. The viability of cells treated with HCLR decreased to 63%, lower than that of HLR (81%) and LR (66.3%). The negative control groups of HCLR and HLR both exhibited cell viability ~95%. 3. Tumor size in the HLR group was nearly 2-times larger than that of the HCLR group, while tumor size in LR and saline groups were nearly 4-times larger.	(*162*)
Magnetic	Oct and Fe_3O_4 MNPs	OA	Human lung carcinoma (A549) cells and cervical carcinoma (HeLa) cells	Female Kunming mice	1. The mean inhibition rates of OA-lips, OA-Olips and OA-OMlips in A549 cells were 82.51, 90.06 and 89.76%, respectively. There was no significant difference for HeLa cells under the same conditions, their mean inhibition rates were 83.82, 85.18 and 84.68%, respectively. 2. The growth of the tumors was significantly inhibited in the OA-OMlips (with magnet) group compared with the groups treated with other formulations.	(*163*)
Redox	ES and COS	DOX	osteosarcoma (MG63) cells and liver (LO2) cells	Male BALB/c nude mice	1. The cellular uptake rates were ranked in order: free DOX > Chol-SS-COS/ES-Lp > Chol-SS-COS-Lp > Chol-COS-Lp for both cells. 2. The tumor weights (g) were measured as 2.84 ± 0.23, 1.90 ± 0.16, 1.38 ± 0.13, 1.12 ± 0.02 and 0.70 ± 0.12 for the groups treated with normal saline, free DOX, Chol-COS-Lp, Chol-SS-COS-Lp and Chol-SS-COS/ES-Lp, respectively.	(*164*)

Stimuli	Moiety	Payload	Cancer cell line	Animal model	Main findings	Ref.
NIR light and Temperature	FA	Au NRs and DOX	Mouse breast cancer (4T1) cells and mouse origin fibroblast (NIH3T3) cells	Balb/c mice	1. 5 min NIR pulses triggered DOX release, reaching 46.38% in 60 min at pH 5.5.	(*165*)
NIR light and Magnetic	HA	DTX and citric acid coated MNPs	Breast cancer (MCF-7) cells and mouse origin fibroblast (NIH3T3) cells	n/a	1. Under NIR irradiation the HA-MNP-LPs released over 20% more drug than the non-irradiated liposomes. 2. The IC_{50} values of free DTX, DTX/MNP-LPs, DTX/HA-MNP-LPs and the irradiated group were 8.93 ± 2.64 µg/mL, 2.37 ± 0.18 µg/mL, 414 1.35 ± 0.34 µg/mL, and 0.69 ± 0.10 µg/mL respectively.	(*166*)
US	RGD, HSA and ES	Calcein	n/a	n/a	1. The results suggest that the AKF is adept at handling drug release estimation problems with a priori unknown or with changing noise covariances. 2. The AKF approach exhibited a 69% reduction in the level of error in estimating the drug release state.	(*167*)
US	Tf, RGD and HSA	Calcein	n/a	n/a	1. Pegylated liposomes were more sonosensitive compared to nonpegylated liposomes when exposed to LFUS. 2. HSA-PEG and Tf-PEG liposomes were more sonosensitive compared to the control pegylated liposomes upon exposure to LFUS.	(*168*)
US	Folate	PFC5 emulsions, Calcein and model GFP plasmid	Cervial carcinoma (HeLa) cells	n/a	1. The application of LFUS enhanced the drug delivery and plasmid transfection. 2. Delivery of therapeutics appears was to the cytosol, indicating that the expansion of the emulsion droplets disrupted both the eLiposomes and the endosomes.	(*169*)
US	HA	Calcein	Breast cancer cell line (MDA-MB-231 and NIH-3T3, an embryonic mouse fibroblast,	n/a	1. LFUS triggered HA liposomes showed a significant enhancement of calcein uptake by MDA-MB-231 cells compared to calcein uptake without US.	(*170*)
Temperature and magnetic	MAB1031 antibody	DOX and Gadolinium-chelate	Breast cancer (MDA-MB-231) cells	n/a	1. DOX release from $Lip_{TS-GD-MAB}$ at 37 °C, was about 21.7 ± 3% after 24 h. 2. DOX release at (39–40 °C) was rapid reaching about 78% and 88% after 1 h, respectively. 3. Increase in fluorescence after treatment with $Lip_{TS-GD-MAB}$ was observed, indicating effective cellular binding.	(*171*)

Stimuli	Moiety	Payload	Cancer cell line	Animal model	Main findings	Ref.
pH	FRβ	Doxycycline (anti-CAPN2) and DTX	Lung adenocarcinoma (PC-9, NCI-H1650 and A549-Luc) cells	Male Balb/c nude mice	1. After treatment with A549-Luc cells, the FRβ-pH lipo-Cy5.5 showed 7.23- and 10.93-fold stronger fluorescence signals compared to NH_2-pH lipo-Cy5.5 and control, respectively. 2. *In vivo*, the DTXL/DOXY lipo-treated group showed a significant tumor growth inhibitory effect compared to the other treatment groups.	(*172*)
US	FA	MnP	Mouse breast cancer (4T1) cells	Female Balb/c mice	1. FA-MnPs showed higher cellular uptake than MnPs. 2. 85% of 4T1 cells in the FA-MnPs + US group were killed, suggesting excellent SDT effect. 3. Strong $^1O_2$ signal occurred in the right tumor in FA-MnPs + US(s) group, suggesting good SDT efficiency of FA-MnPs, while no obvious $^1O_2$ signal was observed in the left tumor (no US treatment). 4. Tumors in FA-MnPs + US groups were effectively suppressed due to efficient SDT.	(*173*)

Abbreviations: **CET**, Cetuximab; **HA-g-DEAP**, Hyaluronic acid grafted with functional 3-diethylaminopropyl; **DTX**, Docetaxel; **GGLG**, 1,5-Dihexadecyl N,N-diglutamyl-lysyl-L-glutamate ; **^{111}In-EGF**, Indium-111 tagged epidermal growth factor; **HSA**, Human serum albumin; ES, Estrone; **HA**, Hyaluronic acid; **ACPP**, Activatable cell penetrating peptide; **PTX**, Paclitaxel; **MMP**, Matrix metalloproteinase; **LPDp**, Polymer-liposomes grafted with anti-PD-L1 peptide and loaded with DOX; **LPp**, Polymer liposomes grafted with peptide; **IL-2**, Interleukin-2; **PD-L1**, Programmed cell death ligand 1 antibody; **IQ**, Imiquimod; **CS**, Chitosan; **HAase**, Permeation promoter hyaluronidase; **LR**, DOTAP/survivin-shRNA; **LPR**, CS/DOTAP/survivin-shRNA lipopolyplex; **CLR**, HAase/CS/DOTAP/survivin-shRNA; **HCLR**, HA/HAase/CS/liposome/survivin-shRNA; **OMlips**, Octreotide-modified magnetic liposomes; **Oct**, Octreotide; **ES**, Estrogen; **COS**, Chotooligosaccharides; **ICG**, Indocyanine green; **poly I:C**, Polyinosinic:polycytidylic acid; **FA**, Folic acid, **Au NRs**, Gold nanorods; **CPT-11**, Camptosar; **AKF**, Adaptive Kalman filter; **LFUS**, Low-frequency ultrasound; **MnP**, Manganese-protoporphyrin.